

# Performance Evaluation of Arizona's LTPP SPS-9 Project: Strategic Study of Flexible Pavement Binder Factors



Arizona Department of Transportation Research Center



# **Performance Evaluation of Arizona's LTPP SPS-9 Project: Strategic Study of Rehabilitation of Flexible Pavement Binder Factors**

**SPR-396-9A  
June 2015**

**Prepared by:**

Jason Puccinelli  
Nichols Consulting Engineers  
1885 S. Arlington Avenue, Suite 111  
Reno, NV 89509-3370

Steven M. Karamihas  
The University of Michigan Transportation Research Institute  
2901 Baxter Road  
Ann Arbor, MI 48109

Kathleen T. Hall  
Kathleen T. Hall Consulting  
1271 Huntington Drive South  
Mundeleine, IL 60060

Jonathan Minassian  
Kevin Senn  
Nichols Consulting Engineers  
1885 S. Arlington Avenue, Suite 111  
Reno, NV 89509-3370

**Published by:**

Arizona Department of Transportation  
206 S. 17th Avenue  
Phoenix, AZ 85007  
in cooperation with  
US Department of Transportation  
Federal Highway Administration

This report was funded in part through grants from the Federal Highway Administration, U.S. Department of Transportation. The contents of this report reflect the views of the authors, who are responsible for the facts and the accuracy of the data, and for the use or adaptation of previously published material, presented herein. The contents do not necessarily reflect the official views or policies of the Arizona Department of Transportation or the Federal Highway Administration, U.S. Department of Transportation. This report does not constitute a standard, specification, or regulation. Trade or manufacturers' names that may appear herein are cited only because they are considered essential to the objectives of the report. The U.S. government and the State of Arizona do not endorse products or manufacturers.

1. Report No. FHWA-AZ-15-396(9A)		2. Government Accession No.		3. Recipient's Catalog No.	
4. Title and Subtitle Performance Evaluation of Arizona's LTPP SPS-9 Project: Strategic Study of Flexible Pavement Binder Factors				5. Report Date June 2015	
				6. Performing Organization Code	
7. Author(s) Jason Puccinelli, Steven Karamihas, Kathleen T. Hall, Jonathan Minassian, Kevin Senn				8. Performing Organization Report No.	
9. Performing Organization Name and Address Nichols Consulting Engineers 1885 South Arlington Avenue Suite 111 Reno, Nevada 89509-3370  The University of Michigan Transportation Research Institute 2901 Baxter Road Ann Arbor, Michigan 48109				10. Work Unit No. (TRAIS)	
				11. Contract or Grant No. SPR 000-147 (396) 9A	
12. Sponsoring Agency Name and Address Arizona Department of Transportation 206 S. 17th Avenue Phoenix, Arizona 85007				13. Type of Report and Period Covered	
				14. Sponsoring Agency Code	
15. Supplementary Notes  Prepared in cooperation with the US Department of Transportation, Federal Highway Administration					
16. Abstract As part of the Long Term Pavement Performance (LTPP) Program, the Arizona Department of Transportation (ADOT) constructed eight Specific Pavement Studies 9 (SPS-9) test sections on Interstate 10 near Phoenix (04B900). SPS-9A 04B900 is an overlay project and is accordingly given independent analysis and documentation in this report separate from Arizona SPS-9B projects (040900 and 04A900) located on US 93, which were new construction and are documented in a separate report. The SPS-9A project studied the effect of asphalt specification and mix designs on flexible pavements, specifically comparing Superpave binders with commonly used agency binders. Opened to traffic in 1995, the project was monitored at regular intervals until it was rehabilitated in 2005. Surface distress, profile, and deflection data collected throughout the life of the pavement were used to evaluate the performance of various flexible pavement design features, layer configurations, and thickness. This report documents the analyses conducted as well as practical findings and lessons learned that will be of interest to ADOT.					
17. Key Words LTPP, pavement performance, profile, distress, FWD, flexible, AC, deflections, roughness, backcalculation		18. Distribution Statement Document is available to the U.S. public through the National Technical Information Service, Springfield, VA 22161		23. Registrant's Seal	
19. Security Classification Unclassified	20. Security Classification Unclassified	21. No. of Pages 82	22. Price		

# SI\* (MODERN METRIC) CONVERSION FACTORS

## APPROXIMATE CONVERSIONS TO SI UNITS

Symbol	When You Know	Multiply By	To Find	Symbol
<b>LENGTH</b>				
in	inches	25.4	millimeters	mm
ft	feet	0.305	meters	m
yd	yards	0.914	meters	m
mi	miles	1.61	kilometers	km
<b>AREA</b>				
in <sup>2</sup>	square inches	645.2	square millimeters	mm <sup>2</sup>
ft <sup>2</sup>	square feet	0.093	square meters	m <sup>2</sup>
yd <sup>2</sup>	square yard	0.836	square meters	m <sup>2</sup>
ac	acres	0.405	hectares	ha
mi <sup>2</sup>	square miles	2.59	square kilometers	km <sup>2</sup>
<b>VOLUME</b>				
fl oz	fluid ounces	29.57	milliliters	mL
gal	gallons	3.785	liters	L
ft <sup>3</sup>	cubic feet	0.028	cubic meters	m <sup>3</sup>
yd <sup>3</sup>	cubic yards	0.765	cubic meters	m <sup>3</sup>
NOTE: volumes greater than 1000 L shall be shown in m <sup>3</sup>				
<b>MASS</b>				
oz	ounces	28.35	grams	g
lb	pounds	0.454	kilograms	kg
T	short tons (2000 lb)	0.907	megagrams (or "metric ton")	Mg (or "t")
<b>TEMPERATURE (exact degrees)</b>				
°F	Fahrenheit	5 (F-32)/9 or (F-32)/1.8	Celsius	°C
<b>ILLUMINATION</b>				
fc	foot-candles	10.76	lux	lx
fl	foot-Lamberts	3.426	candela/m <sup>2</sup>	cd/m <sup>2</sup>
<b>FORCE and PRESSURE or STRESS</b>				
lbf	poundforce	4.45	newtons	N
lbf/in <sup>2</sup>	poundforce per square inch	6.89	kilopascals	kPa

## APPROXIMATE CONVERSIONS FROM SI UNITS

Symbol	When You Know	Multiply By	To Find	Symbol
<b>LENGTH</b>				
mm	millimeters	0.039	inches	in
m	meters	3.28	feet	ft
m	meters	1.09	yards	yd
km	kilometers	0.621	miles	mi
<b>AREA</b>				
mm <sup>2</sup>	square millimeters	0.0016	square inches	in <sup>2</sup>
m <sup>2</sup>	square meters	10.764	square feet	ft <sup>2</sup>
m <sup>2</sup>	square meters	1.195	square yards	yd <sup>2</sup>
ha	hectares	2.47	acres	ac
km <sup>2</sup>	square kilometers	0.386	square miles	mi <sup>2</sup>
<b>VOLUME</b>				
mL	milliliters	0.034	fluid ounces	fl oz
L	liters	0.264	gallons	gal
m <sup>3</sup>	cubic meters	35.314	cubic feet	ft <sup>3</sup>
m <sup>3</sup>	cubic meters	1.307	cubic yards	yd <sup>3</sup>
<b>MASS</b>				
g	grams	0.035	ounces	oz
kg	kilograms	2.202	pounds	lb
Mg (or "t")	megagrams (or "metric ton")	1.103	short tons (2000 lb)	T
<b>TEMPERATURE (exact degrees)</b>				
°C	Celsius	1.8C+32	Fahrenheit	°F
<b>ILLUMINATION</b>				
lx	lux	0.0929	foot-candles	fc
cd/m <sup>2</sup>	candela/m <sup>2</sup>	0.2919	foot-Lamberts	fl
<b>FORCE and PRESSURE or STRESS</b>				
N	newtons	0.225	poundforce	lbf
kPa	kilopascals	0.145	poundforce per square inch	lbf/in <sup>2</sup>

\*SI is the symbol for the International System of Units. Appropriate rounding should be made to comply with Section 4 of ASTM E380. (Revised March 2003)

## Contents

<b>EXECUTIVE SUMMARY .....</b>	<b>1</b>
<b>CHAPTER 1. INTRODUCTION .....</b>	<b>3</b>
<b>CHAPTER 2. SPS-9A DEFLECTION ANALYSIS .....</b>	<b>15</b>
ANALYSIS OF DEFLECTION DATA.....	15
MAXIMUM DEFLECTION, MINIMUM DEFLECTION, AND AREA VALUE.....	15
BACKCALCULATION PROCEDURE .....	19
BACKCALCULATION USING EVERCALC SOFTWARE .....	23
KEY FINDINGS FROM THE SPS-9A DEFLECTION ANALYSIS .....	26
<b>CHAPTER 3. SPS-9A DISTRESS ANALYSIS .....</b>	<b>29</b>
AC DISTRESS TYPES.....	29
RESEARCH APPROACH.....	30
OVERALL PERFORMANCE TREND OBSERVATIONS.....	32
KEY FINDINGS FROM THE SPS-9A DISTRESS ANALYSIS .....	39
<b>CHAPTER 4. SPS-9A ROUGHNESS ANALYSIS.....</b>	<b>41</b>
PROFILE DATA SYNCHRONIZATION.....	41
DATA EXTRACTION .....	42
CROSS CORRELATION .....	42
SYNCHRONIZATION .....	43
DATA QUALITY SCREENING .....	43
SUMMARY ROUGHNESS VALUES .....	47
PROFILE ANALYSIS TOOLS .....	52
DETAILED OBSERVATIONS.....	54
SUMMARY .....	64
<b>CHAPTER 5. CONCLUSIONS AND RECOMMENDATIONS .....</b>	<b>69</b>
<b>REFERENCES.....</b>	<b>71</b>
<b>APPENDIX: ROUGHNESS VALUES .....</b>	<b>73</b>

## List of Figures

Figure 1.	Existing Pavement Structure for the SPS-9A Project.....	4
Figure 2.	Pavement Structure for the SPS-9A Project After Construction .....	4
Figure 3.	Layout of the SPS-9A Test Sections .....	5
Figure 4.	SPS-9A Test Section Layout .....	6
Figure 5.	Location of SPS-9A 04B900 Test Sections .....	7
Figure 6.	Gradations of Superpave Aggregate and Agency Standard Aggregate.....	12
Figure 7.	Average Normalized $D_{max}$ by Test Section .....	16
Figure 8.	Average Normalized $D_{min}$ by Test Section .....	17
Figure 9.	AREA Values by Test Section .....	19
Figure 10.	Backcalculated AC Modulus by Test Section .....	25
Figure 11.	Backcalculated $M_R$ by Test Section .....	26
Figure 12.	Structural Damage Trends for SPS-9A Test Sections.....	33
Figure 13.	Environmental Damage Trends for SPS-9A Test Sections.....	34
Figure 14.	Structural Damage Index and Pavement Structure Summary .....	35
Figure 15.	Environmental Damage Index and Pavement Structure Summary .....	36
Figure 16.	Rutting Index and Pavement Structure Summary.....	37
Figure 17.	IRI Progression of Section 04B901.....	48
Figure 18.	IRI Progression of Section 04B902.....	48
Figure 19.	IRI Progression of Section 04B903.....	49
Figure 20.	IRI Progression of Section 04B959.....	49
Figure 21.	IRI Progression of Section 04B960.....	50
Figure 22.	IRI Progression of Section 04B961.....	50
Figure 23.	IRI Progression of Section 04B962.....	51
Figure 24.	IRI Progression of Section 04B964.....	52
Figure 25.	Summary of IRI Ranges.....	66
Figure 26.	Comparison of HRI to MRI.....	74

## List of Tables

Table 1.	SPS-9A Site Structural Factors .....	3
Table 2.	SPS-9A Mix Properties (As Designed) .....	9
Table 3.	SPS-9A Mix Properties (As Constructed) .....	10
Table 4.	Dynamic Modulus ( $E^*$ ) for Test Section 041007/04B962 .....	11
Table 5.	Climatic Information for SPS-9A .....	12
Table 6.	SPS-9A Traffic-Loading Summary .....	13
Table 7.	General Trends of $D_0$ and Area Values .....	18
Table 8.	Structural Parameter Statistics for SPS-9A .....	22
Table 9.	Backcalculation Seed Value and Modulus Range .....	23
Table 10.	Backcalculation Moduli Statistics for SPS-9A Test Sections .....	24
Table 11.	Flexible Pavement Distress Types and Failure Mechanisms .....	30
Table 12.	Profile Measurement Visits of the SPS-9A Site .....	41
Table 13.	Selected Repeats of Section 04B901 .....	44
Table 14.	Selected Repeats of Section 04B902 .....	44
Table 15.	Selected Repeats of Section 04B903 .....	44
Table 16.	Selected Repeats of Section 04B959 .....	45
Table 17.	Selected Repeats of Section 04B960 .....	45
Table 18.	Selected Repeats of Section 04B961 .....	45
Table 19.	Selected Repeats of Section 04B962 .....	45
Table 20.	Selected Repeats of Section 04B964 .....	46
Table 21.	Roughness Values .....	74

## List of Acronyms and Abbreviations

AASHTO	American Association of State Highway and Transportation Officials
AB	aggregate base
AC	asphalt concrete
ACFC	asphalt concrete friction course
ADOT	Arizona Department of Transportation
ARAC	asphalt rubber asphalt concrete
COV	coefficient of variation
$D_{\max}$	maximum deflection
$D_{\min}$	minimum deflection
$E^*$	dynamic modulus
$E_p$	effective pavement modulus
ESAL	equivalent single axle load
FWD	falling weight deflectometer
HRI	Half-car Roughness Index
I-10	Interstate 10
IRI	International Roughness Index
ksi	kips per square inch
lbf	pound force
LTPP	Long Term Pavement Performance
$M_R$	resilient modulus
MP	milepost
MRI	Mean Roughness Index
NWP	non-wheelpath
PCC	portland cement concrete
PSD	power spectral density
psi	pounds per square inch
RN	Ride Number
SMA	stone mastic asphalt
SN	structural number
$SN_{\text{eff}}$	effective structural number
SP-I	Superpave, Level I
SP-III	Superpave, Level III
SPS	Specific Pavement Studies
WP	wheelpath

## **Acknowledgments**

The project team would like to acknowledge the Arizona Department of Transportation (ADOT) for sponsoring this project. In addition, the authors thank the ADOT Research Center and the Technical Advisory Committee for their input as well as the leadership of Christ Dimitroplos. Larry Scofield's contribution to the report is also greatly appreciated. The comprehensive information stored in the Long Term Pavement Performance database allowed for this research to be conducted.



## EXECUTIVE SUMMARY

As part of the Long Term Pavement Performance (LTPP) Program, the Arizona Department of Transportation (ADOT) constructed eight Specific Pavement Studies 9 (SPS-9) test sections on Interstate 10 near Phoenix, identified herein as SPS-9A. The SPS-9A project studied the effect of asphalt specification and mix designs on flexible pavements, specifically comparing Superpave binders with commonly used agency binders. Each of the eight SPS-9A (04B900) sections received the same basic rehabilitation using different materials as part of the standard experiment. These sections had the same structural properties before receiving the mill and overlay treatment. Construction of all eight sections occurred in March 1995, and they were placed out of study in February 2005 when the sections were milled and overlaid.

This report provides general information about the project location, including climate, traffic, and subgrade conditions, as well as details about the mix designs of each test section. All eight of the SPS-9A test sections were constructed consecutively and exposed to the same traffic-loading, climate, and subgrade conditions, which allowed for direct comparisons between mix design performance without the confounding effects introduced by different in situ conditions.

Most sections had a clear increase in magnitude of environmental distress approximately 10 years after construction. Where fatigue cracking was very prevalent, it was difficult to match individual cracks to roughness within the measured profile. However, in a few cases, features in the profiles that affected the roughness were found that correspond directly to the location of transverse cracks noted in the distress survey.

From a roughness perspective, the stone mastic asphalt (SMA) cellulose and asphalt rubber asphalt concrete sections outperformed the Superpave mixes. Considering all distresses, the SMA cellulose significantly outperformed the other sections of this project.

The vast majority of sections showed significant growth in longitudinal and, consequently, fatigue cracking. This significant growth in cracking was observed in the final distress survey, which implies that the growth occurred in between the last two surveys, seven to 10 years after the sections were constructed, with the rate of crack growth slowly increasing until the sections were placed out of study. All sections performed well with regard to rut resistance. Rutting would not have triggered a rehabilitation event for any section.



## CHAPTER 1. INTRODUCTION

Understanding how design features contribute to long-term pavement performance can be extremely valuable to pavement designers looking to optimize resources and improve overall performance. This study’s objectives were to document the overall performance trends of the Specific Pavement Studies 9 (SPS-9) project, identify key differences in performance between the various asphalt specifications and mix designs, and document key findings that would be useful to the Arizona Department of Transportation (ADOT).

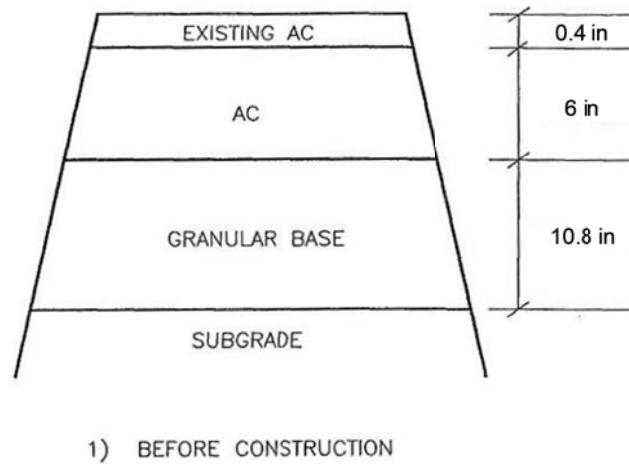
This report provides the results of surface distress, deflection, and profile analyses for the Long Term Pavement Performance (LTPP) SPS-9 project on Interstate 10 (I-10) near Phoenix. SPS-9 sites were designed to study the effect of asphalt specification and mix designs on flexible pavements, specifically comparing Superpave binders with commonly used agency binders. The SPS-9A site (04B900) consisted of eight existing sections that each received the same basic rehabilitation using different materials. These sections had the same structural properties before receiving the mill and overlay treatment.

Table 1 summarizes the structural design of the test sections. All test sections had approximately the same thickness; the LTPP construction report (FHWA 1998) provides more detail about the layout and structural properties of the site.

**Table 1. SPS-9A Site Structural Factors**

Section	Existing Asphalt Concrete Layer Thickness (inches)	Standard Asphalt Concrete Layer Thickness (inches)	Experimental Asphalt Concrete	
			Layer Thickness (inches)	Type
04B901	2.8	4.4	3.5	Agency standard
04B902	3.4	4.4	3.0	Superpave, Level I (SP-1) (PG 76-10)
04B903	3.0	4.4	4.0	SP-1 (PG 70-10)
04B959	2.5	4.5	3.0	Stone mastic asphalt (SMA) polymer with asphalt concrete friction course
04B960	2.5	4.5	3.0	SMA polymer
04B961	2.5	4.5	3.0	SMA cellulose
04B964	2.5	4.5	3.0	Asphalt rubber asphalt concrete
041007/ 04B962	3.6	4.3	2.9	Superpave, Level III

Each test section was resurfaced in March 1995. The resurfacing treatment consisted of milling 4 inches from the existing pavement, placing a 4-inch standard (1.5-inch maximum aggregate) asphalt concrete (AC) layer, and then overlaying with 3 inches of the experimental surfaces, as shown in Figures 1 and 2. The test sections were located entirely on a shallow fill of native material. The subgrade and embankment material are coarse-grained silty sands with gravel and cobbles.



**Figure 1. Existing Pavement Structure for the SPS-9A Project**

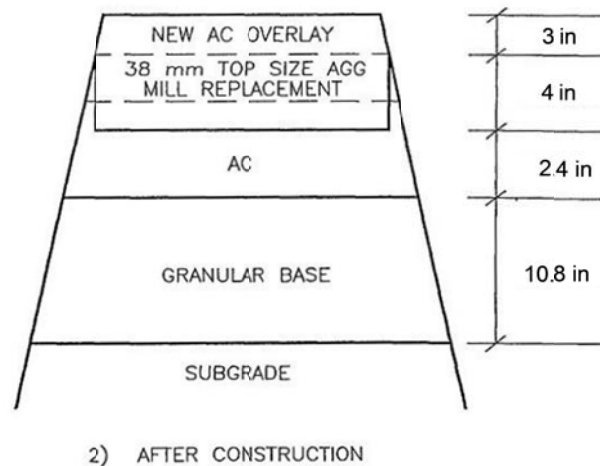


**Figure 2. Pavement Structure for the SPS-9A Project After Construction**

The site extended from milepost (MP) 112.81 to MP 122.29 on westbound I-10. The site is located at latitude 33°27'45" and longitude -112°28'10", with an approximate elevation of 1059 ft. The terrain surrounding the test section is slightly rolling and the roadway is straight. Figures 3 through 5 illustrate the test sections located within the SPS-9A project.

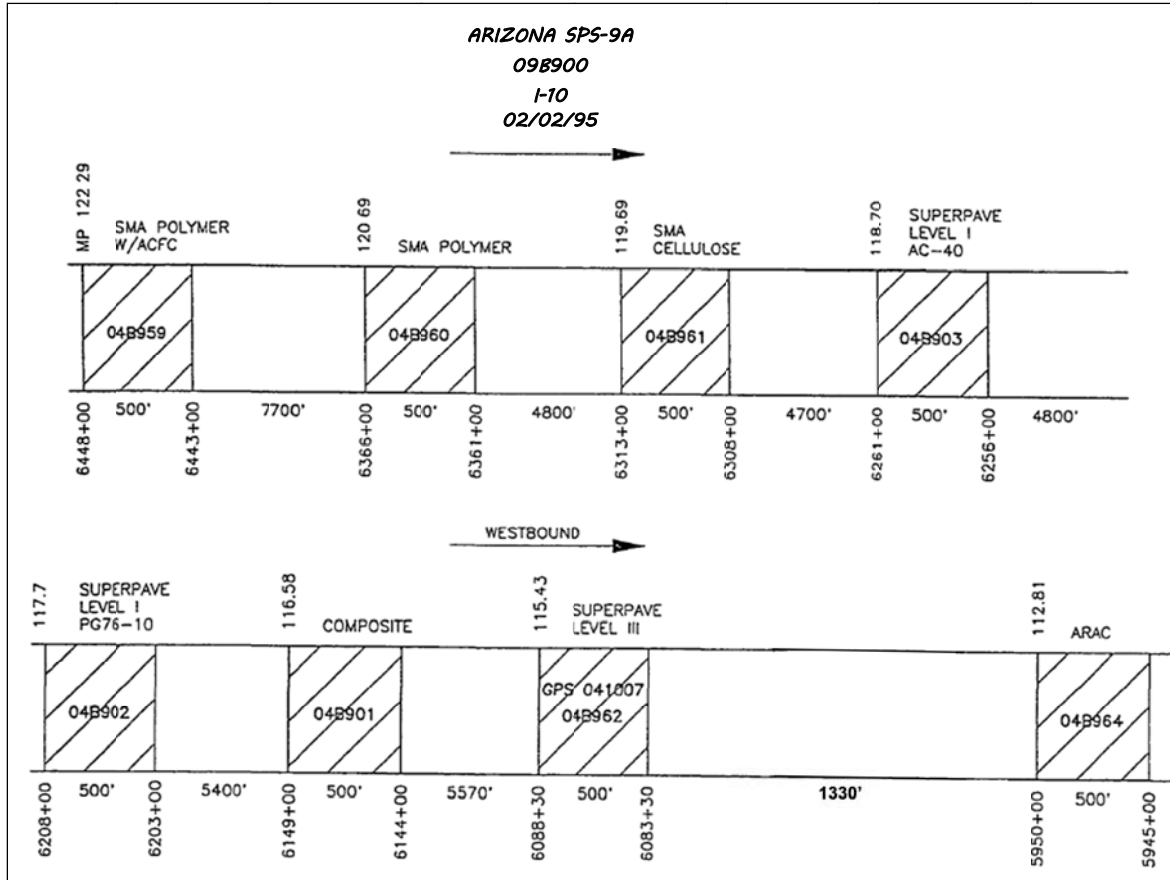


Figure 3. Layout of the SPS-9A Test Sections

Station	Distance	SHRP ID	Original Pavement Configuration						
			AC			Base and Subbase		Base and Subbase	
(ft)	(m)		Thick	Type	Mix Design	Binder Grade	Thick (in)	Type	Type
5945+00	152.4	04B964	0.5	Open Grade AC	ARAC		10.8	Crushed Gravel	Coarse Grained Soil: Silty Sand with Gravel
5950+00			6.5	Dense Grade AC					
6083+30	152.4	04B962/ 041007	0.5	Open Grade AC	Superpave Level III		10.8	Crushed Gravel	Coarse Grained Soil: Silty Sand with Gravel
6088+30			6.0	Dense Grade AC					
6144+00	152.4	04B901	0.5	Open Grade AC	ADOT Standard (Marshall Design)	PG 76-10	10.8	Crushed Gravel	Coarse Grained Soil: Silty Sand with Gravel
6149+00			6.8	Dense Grade AC					
6203+00	152.4	04B902	0.5	Open Grade AC	Superpave Level I: 1 in (25mm)	PG 76-10	10.8	Crushed Gravel	Coarse Grained Soil: Silty Sand with Gravel
6208+00			7.4	Dense Grade AC					
6256+00	152.4	04B903	0.5	Open Grade AC	Superpave Level I: 1 in (25mm)	AC-40 (=PG 70-10)	10.8	Crushed Gravel	Coarse Grained Soil: Silty Sand with Gravel
6261+00			7.0	Dense Grade AC					
6308+00	152.4	04B961	0.5	Open Grade AC	SMA Cellulose		10.8	Crushed Gravel	Coarse Grained Soil: Silty Sand with Gravel
6313+00			6.5	Dense Grade AC					
6361+00	152.4	04B960	0.5	Open Grade AC	SMA Polymer		10.8	Crushed Gravel	Coarse Grained Soil: Silty Sand with Gravel
6366+00			6.5	Dense Grade AC					
6443+00	152.4	04B959	0.5	Open Grade AC	SMA Polymer with ACFC		10.8	Crushed Gravel	Coarse Grained Soil: Silty Sand with Gravel
6448+00			6.5	Dense Grade AC					

Figure 4. SPS-9A Test Section Layout



**Figure 5. Location of SPS-9A 04B900 Test Sections  
(Courtesy of Google Maps)**

Of the eight experimental sections, three are specifically for the SPS-9A experiment: 04B901, 04B902, and 04B903. 04B901 is a standard agency mix design using the Marshall 75 blow mix design. 04B902 and 04B903 are Superpave, Level 1 (SP-1) mixes that used PG 76-10 and AC-40 (PG 70-10) binders, respectively. When using the LTPP Bind 3.1 software, the recommended binder for this project site was PG 76-10. The following inputs were used in the program:

- Latitude: 33.46 degrees.
- Lowest yearly air temperature: -4.5° C.
- Yearly degree-days greater than 10° C: 5387.
- Low air temperature standard deviation: 2.2° C.
- Desired reliability: 98 percent.
- Depth of layer: 0 mm.
- Traffic speed: Fast.
- Traffic loading: Up to 3 million equivalent single axle loads (ESALs).

The SPS-9A experiment also included five supplemental test sections: 04B959, 04B960, 04B961, 04B964, and 041007/04B962. Sections 04B959, 04B960, and 04B961 were stone mastic asphalt (SMA) pavements. Section 04B959 was an SMA polymer with an asphalt concrete friction course (ACFC); 04B960 was an SMA polymer pavement; and 04B961 was an SMA cellulose pavement. Section 04B964 was an asphalt rubber asphalt concrete (ARAC) pavement. All mixtures included Type II portland cement concrete (PCC) as an admixture. Although eight experimental sections were constructed, time and budget constraints did not allow for detailed information to be recorded on the supplemental sections.

The aggregate properties of Superpave sections 04B902 and 04B903 follow:

- Bulk specific gravity of aggregate: 2.672.
- Bulk specific gravity of admixture: 3.140.
- Bulk specific gravity of the total gradation: 2.677.
- Effective specific gravity of the total gradation: 2.712.

Table 2 provides the design mix properties and Table 3 provides the construction mix properties for the SPS-9A test sections.

**Table 2. SPS-9A Mix Properties (As Designed)**

	<b>04B901</b>	<b>04B902</b>	<b>04B903</b>	<b>04B960</b>	<b>04B961</b>	<b>All Sections</b>
<b>Layer</b>	Agency mix	SP-1 (PG 76-10)	SP-1 (PG 70-10)	SMA polymer	SMA cellulose	Standard AC below experimental layer
Mix type	Marshall	Superpave	Superpave	N/A	N/A	N/A
Maximum specific gravity	N/A	2.532	2.532	N/A	N/A	N/A
Bulk specific gravity	2.368	2.425	2.426	N/A	N/A	N/A
Asphalt content (%)	3.8	4.3	4.3	5.2	5.3	3.4
Air voids (%)	6	4.2	4.2	N/A	N/A	N/A
Mineral aggregate air voids (%)	N/A	13.3	13.3	N/A	N/A	N/A
Effective asphalt content (%)	N/A	3.8	3.8	N/A	N/A	N/A
Number of blows	75	N/A	N/A	N/A	N/A	N/A
Asphalt grade	N/A	N/A	AC-40	AC-40	N/A	N/A
PG high temperature (°C)	76	76	70	N/A	N/A	N/A
PG low temperature (°C)	10	10	10	N/A	N/A	N/A
Maximum particle size (mm)	N/A	25.4	25.4	N/A	N/A	N/A
Bulk density (kg/m <sup>3</sup> )	2368	N/A	N/A	N/A	N/A	N/A
Rice density (kg/m <sup>3</sup> )	2483	N/A	N/A	N/A	N/A	N/A
Avg. (M <sub>R</sub> ) at 5° C	N/A	15.663	N/A	N/A	N/A	19.134
Avg. (M <sub>R</sub> ) at 25° C	N/A	9.27	N/A	N/A	N/A	11.068
Avg. (M <sub>R</sub> ) at 40° C	N/A	2.743	N/A	N/A	N/A	3.52

N/A: Not available.

**Table 3. SPS-9A Mix Properties (As Constructed)**

	<b>04B901</b>		<b>04B902</b>		<b>04B903</b>	<b>04B961</b>	
<b>Layer</b>	Standard AC layer	Agency mix	Standard AC layer	SP-1 (PG 76-10)	Standard AC layer	Standard AC layer	SMA cellulose
Mix type	N/A	N/A	N/A	Superpave	N/A	N/A	N/A
Bulk specific gravity (mean)	N/A	N/A	2.449	N/A	N/A	N/A	N/A
Bulk specific gravity (minimum)	N/A	N/A	2.265	N/A	N/A	N/A	N/A
Bulk specific gravity (maximum)	N/A	N/A	2.505	N/A	N/A	N/A	N/A
Asphalt content (mean)	3.6	3.7	3.4	4.1	3.3	3.6	5.1
Asphalt content (minimum)	3.6	3.65	3.2	4.0	3.2	3.5	5.1
Asphalt content (maximum)	3.6	3.75	3.7	4.1	3.5	3.8	5.1
Air voids (mean) (%)	3.8	6.2	3.1	3.8	2.4	2.9	3.6
Air voids (minimum) (%)	3.7	5.55	2.1	3.0	N/A	2.6	3.4
Air voids (maximum) (%)	3.8	7.15	4.1	5.1	N/A	3.1	3.8

N/A: Not available.

The dynamic modulus ( $E^*$ ) was calculated for Section 041007/04B962. The  $E^*$  values provided in Table 4 are estimates based on the resilient modulus Artificial Neural Network model developed in 2011 (Kim et al. 2011).

**Table 4. Dynamic Modulus (E\*) for Test Section 041007/04B962**

Layer	Temperature (°C)	Sample Age (Days)	Frequency					
			0.1	0.5	1	5	10	25
Existing AC	14	44	3694828	4074048	4216398	4500353	4603928	4725184
	40	44	1967348	2497805	2724167	3225375	3425915	3673586
	70	44	532003	834205	994522	1430188	1640226	1931954
	100	44	115027	196541	247269	414452	511889	667432
	130	44	35623	56534	70009	117823	148342	201351
Standard AC	14	135	4330092	4576202	4664152	4832633	4891801	4959504
	40	135	2935557	3421560	3611171	3999767	4144552	4315779
	70	135	1127095	1602026	1826265	2367267	2600349	2900745
	100	135	282964	474572	585666	917717	1092434	1349704
	130	135	79880	134431	169391	289834	363395	485354
SP-3	14	135	4321909	4573729	4664235	4838556	4900125	4970844
	40	135	2919646	3404883	3595022	3986572	4133229	4307322
	70	135	1126592	1597170	1819156	2355060	2586341	2884986
	100	135	283947	476537	587732	918662	1092199	1347284
	130	135	78523	133794	169201	290872	364931	487343
SP-1 (PG 76-10)	14	58	4359022	4612543	4703856	4880106	4942501	5014285
	40	58	2954525	3439803	3630074	4022336	4169478	4344357
	70	58	1155592	1629823	1852780	2389785	2621197	2919867
	100	58	295975	494355	608223	945083	1120821	1378316
	130	58	81971	139875	176830	303140	379601	505439

The gradations for the Superpave and standard agency aggregate are shown in Figure 6. As previously mentioned, some mixture and other data were not available for all test sections.

By LTPP definitions, the SPS-9A project site is a dry, no-freeze environment (Table 5). The temperature and precipitation information in Table 5 represents 40 years of recorded data collected at nearby weather stations. The solar radiation and humidity data were summarized from 15 years of weather station data from the nearby SPS-2 project.

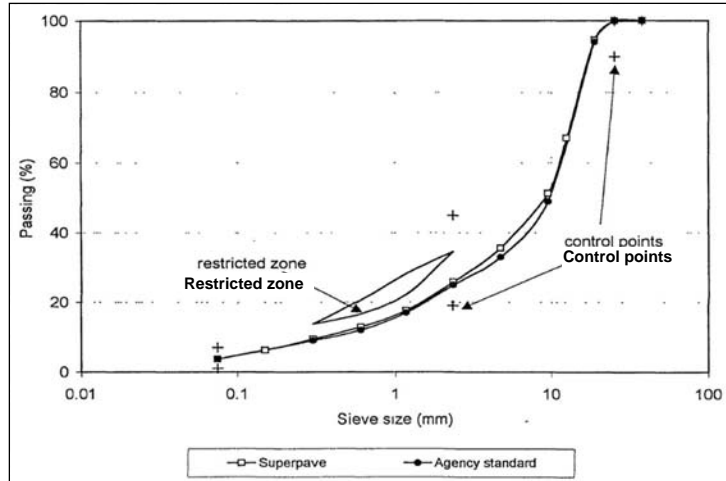


**Figure 6. Gradations of Superpave Aggregate and Agency Standard Aggregate (FHWA 1998)**

**Table 5. Climatic Information for SPS-9A**

	<b>40-Year Average</b>	<b>40-Year Maximum</b>	<b>40-Year Minimum</b>
Annual average daily mean temperature (°F)	72	74	69
Annual average daily maximum temperature (°F)	88	90	85
Annual average daily minimum temperature (°F)	55	60	51
Absolute maximum annual temperature (°F)	116	123	111
Absolute minimum annual temperature (°F)	25	31	17
Number of days per year above 32 °F	176	196	133
Number of days per year below 32 °F	17	43	1
Annual average freezing index (°F-days)	0	0	0
Annual average precipitation (inches)	7.7	15.2	1.8
Annual average daily mean solar radiation (W/ft <sup>2</sup> )	22.7	36.8	1.65
Annual average daily maximum relative humidity (%)	53	64	43
Annual average daily minimum relative humidity (%)	17	22	13

Table 6 summarizes the total ESALs computed from traffic-loading information collected at the SPS-9 site. The ESAL values for 1993 and 1994 are ADOT estimates; no monitoring traffic data were available for this period.

**Table 6. SPS-9A Traffic-Loading Summary**

<b>Year</b>	<b>ESALs</b>
1993	1,400,000*
1994	1,100,000*
1995	1,283,553
1996	1,253,915
1997	1,289,820
1998	1,374,457
1999	954,526
2000	2,786,163
2001	1,702,068
2002	2,581,494
2003	3,062,289
2004	1,446,194
2005	1,229,188

\*ADOT traffic estimates. No monitoring data available.

After experiment surfaces were placed in 1995, the following maintenance activities were performed:

- Section 04B901 (agency mix, PG 76-10): No rehabilitation or maintenance conducted.
- Section 04B902 (SP-1, PG 76-10): Pothole patching in 2003.
- Section 04B903 (SP-1, PG 70-10): No rehabilitation or maintenance conducted.
- Section 04B959 (SMA polymer with ACFC): No rehabilitation or maintenance conducted.
- Section 04B960 (SMA polymer): No rehabilitation or maintenance conducted.
- Section 04B961 (SMA cellulose): No rehabilitation or maintenance conducted.
- Section 04B964 (ARAC): No rehabilitation or maintenance conducted.
- Section 041007/04B962 (SP-3): Pothole patching in 2003.

All test sections were placed out of study because of reconstruction in the summer of 2005 except for Section 041007/04B962, which was placed out of study in 2007.

Three analyses were conducted on the SPS-9A project to evaluate pavement performance: deflection, distress, and profile. The following sections address each analysis, including a description of the research approach along with performance comparisons between test sections, overall trends, a summary of the results, and key findings.

## CHAPTER 2. SPS-9A DEFLECTION ANALYSIS

Falling weight deflectometer (FWD) data provide information about the overall strength (i.e., stiffness) of the pavement structure and individual layers. At the SPS-9A site, researchers used this information to evaluate changes with time or, as in the case of the asphalt-bound layers, temperature, and they performed additional analyses to understand how various design features affect structural performance.

### ANALYSIS OF DEFLECTION DATA

Using the nondestructive FWD deflection testing data, researchers can identify the structural condition of the sections over their service life. In this chapter, three levels of analysis are presented. First, researchers produced the deflection profile plots of maximum deflection ( $D_0$ ), minimum deflection ( $D_7/D_8$ ), and AREA value for all the sections to identify changes in the pavement and subgrade over time. Next, they backcalculated subgrade resilient modulus ( $M_R$ ), effective pavement modulus ( $E_p$ ), and effective structural number ( $SN_{eff}$ ) as outlined in the *AASHTO Guide for Design of Pavement Structures* (AASHTO 1993). Finally, they backcalculated AC modulus and  $M_R$  using industry standard software.

### MAXIMUM DEFLECTION, MINIMUM DEFLECTION, AND AREA VALUE

#### Maximum Deflections

The normalized average maximum deflection ( $D_{max}$ ) ( $D_0$ , measured at the center of the FWD load plate, normalized to a load level of 9000 pounds and an AC mix temperature of 68 °F) typically indicates the total stiffness of the pavement structure (surface and base) and the underlying subgrade. Increases in the normalized average maximum deflection (or  $D_{max}$ ) observed over time may be due to weakening of the pavement structure or weakening of the subgrade.

Figure 7 shows  $D_{max}$  results for each test section from the first round of testing to the last. Except for Section 041007, the first round of testing for all sections was performed in 1995. When this testing was performed, the top lift of the AC layer had not been placed, resulting in the relatively high deflections that were observed throughout the project. The second test was performed in 1997—21 months after construction. As expected,  $D_{max}$  reduced significantly compared to the first round of testing.

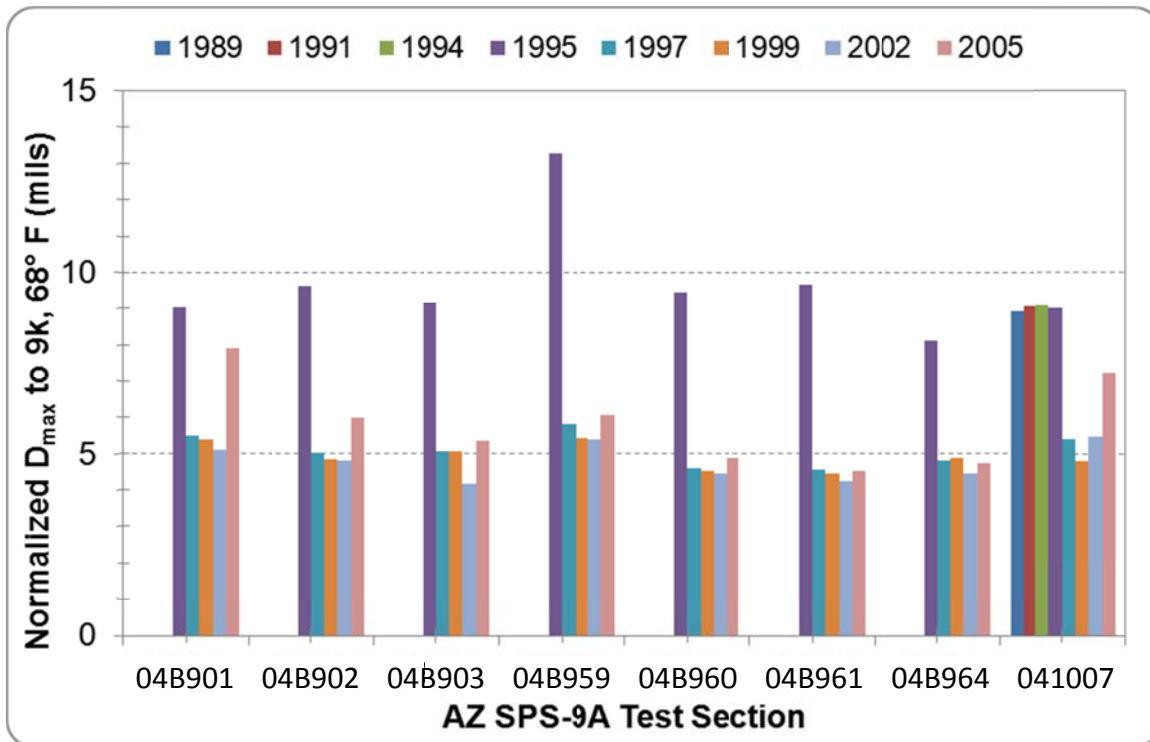


Figure 7. Average Normalized  $D_{max}$  by Test Section

### Minimum Deflection

The minimum deflection ( $D_{min}$ ) was observed in the sensor farthest from the loading plate, which for LTPP can be either sensor No. 7 or sensor No. 8, depending on the configuration used. The  $D_{min}$  readings also normalized to standard 9000 pounds, but no temperature correction factor was applied. The  $D_{min}$  readings were indicative of the subgrade characteristics. Figure 8 shows the  $D_{min}$  measurement from the first round of testing to the last round of testing. In general, subgrade modulus did not change much throughout the test sites. Section 04B964 had the strongest subgrade and Section 04B959 had the weakest subgrade. Interestingly, subgrade strength increased with time in Section 041007.

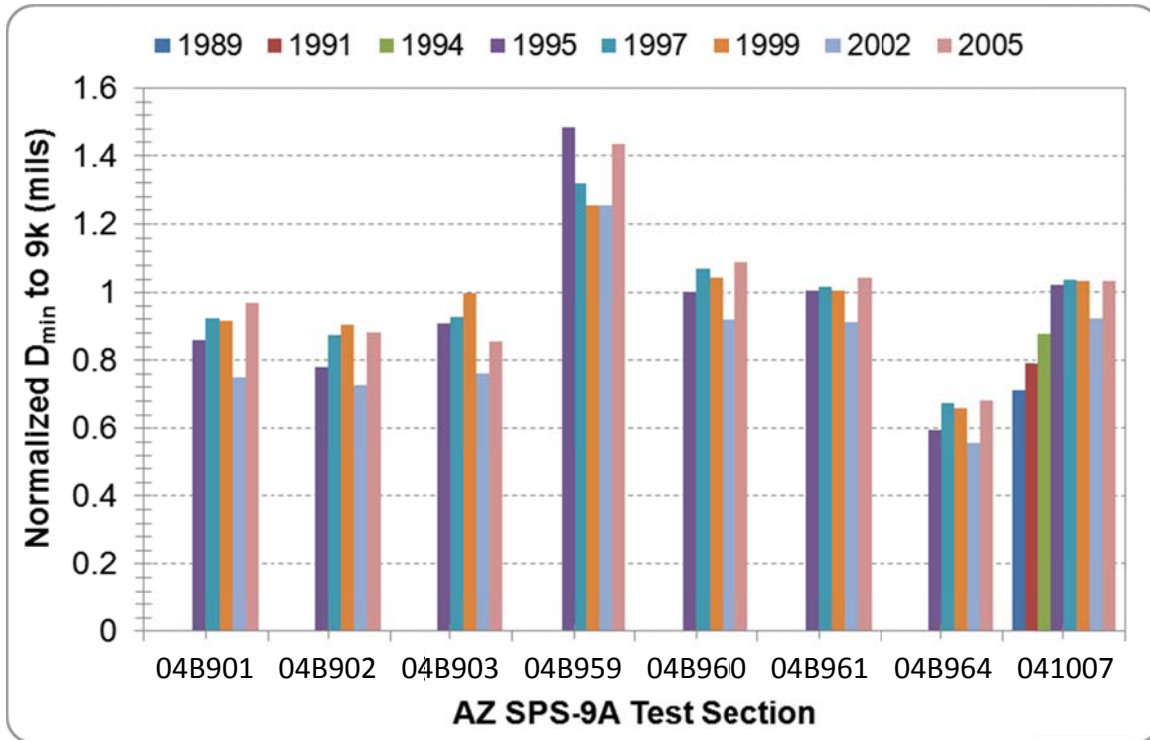


Figure 8. Average Normalized  $D_{min}$  by Test Section

#### AREA Value

The AREA parameter is commonly used as a means of quantifying the relative stiffness of a pavement section. The equation for the AREA value is:

$$A = 6(D_0 + D_1 + D_2 + D_3) / D_0 \quad (\text{Eq. 1})$$

Where  $A$  = AREA value

$D_0$  = surface deflection at center of test load

$D_1$  = surface deflection at 12 inches

$D_2$  = surface deflection at 24 inches

$D_3$  = surface deflection at 36 inches

The AREA value is the normalized area of a slice taken through any deflection basin between the center of the loaded area and 36 inches. This area is said to be normalized because it is divided by the maximum deflection,  $D_0$ . The maximum value of the AREA parameter is 36 inches, which would result from testing an extremely rigid section of pavement, and it occurs when all four deflections are equal. The minimum AREA is 11.02 inches, which would result from deflection measurements on a one-layer system of homogeneous material. This would imply that the pavement structure is of the same stiffness as the underlying soil. The state of Washington suggested that general trends of pavement condition can be concluded from the combination of AREA value and maximum deflection (Table 7) (Mahoney 1995).

**Table 7. General Trends of  $D_0$  and Area Values (Mahoney 1995)**

FWD-Based Parameter		Generalized Conclusions
AREA	$D_{max}$	
Low	Low	Weak structure, strong subgrade
Low	High	Weak structure, weak subgrade
High	Low	Strong structure, strong subgrade
High	High	Strong structure, weak subgrade

Figure 9 shows the average AREA value of the SPS-9A test sections from the first round of testing to the last round of testing. As shown in the figure, a significant increase in AREA value between first and second round of testing was observed, which coincides with the  $D_{max}$  observation.

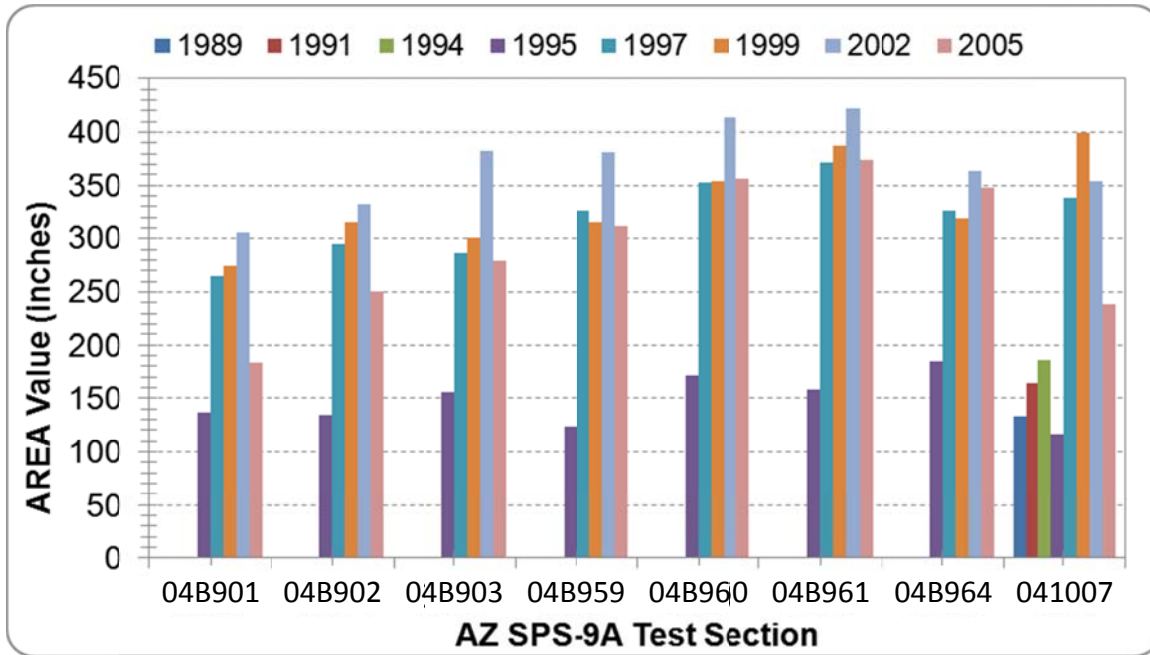


Figure 9. AREA Values by Test Section

#### BACKCALCULATION PROCEDURE

The *AASHTO Guide for Design of Pavement Structures* (1993) outlined a procedure for calculating  $M_R$ , the effective modulus of all pavement layers above the subgrade, and  $SN_{eff}$  using measured deflection data. The deflections, which are measured at a distance at least 0.7 times the radius of the stress bulb at the subgrade-pavement interface, are considered to reflect the deformation of the subgrade layer only and can be used to compute  $M_R$ . The backcalculated  $M_R$  can be calculated as:

$$M_R = \frac{(1 - \mu^2) P}{\pi r D_R} \quad (\text{Eq. 2})$$

Where  $M_R$  = backcalculated subgrade resilient modulus

$\mu$  = Poisson's ratio ( $\mu = 0.5$  was assumed in the analysis)

$P$  = applied load (lbf)

$r$  = distance from center of load plate to  $D_R$  (inches)

$D_R$  = pavement surface deflection at distance  $r$  from the center of the load plate (inches)

The radius of the stress bulb can be determined from the following equation:

$$a_e = \sqrt{a^2 + \left( D^3 \sqrt{\frac{E_p}{M_R}} \right)} \quad (\text{Eq. 3})\#$$

Where  $a_e$  = radius of stress bulb at the subgrade-pavement interface (inches)

$a$  = FWD load plate radius (inches)

$D$  = total thickness of pavement layers (inches)

$E_p$  = effective pavement modulus

$M_R$  = backcalculated subgrade resilient modulus

To obtain  $E_p$  in this equation, the researchers used an equation linking the FWD deflection at the center plate ( $D_{\max}$ ),  $E_p$ , and  $M_R$ :

$$d_0 = 1.5Pa \left[ \frac{1}{M_R \sqrt{1 + \left( \frac{D}{a} \sqrt{\frac{E_p}{M_R}} \right)^2}} + \frac{1 - \frac{1}{\sqrt{1 + \left( \frac{D}{a} \right)^2}}}{E_p} \right] \quad (\text{Eq. 4})\#$$

Where  $d_0$  = deflection at the pavement surface and adjusted to a standard temperature of 68 °F (inches)

$P$  = contact pressure under the loading plate (psi)

$a$  = load plate radius (inches)

$M_R$  = subgrade resilient modulus (psi)

$D$  = actual pavement structure thickness (inches)

$E_p$  = effective modulus of the pavement structure (psi)

Once  $E_p$  was determined,  $SN_{eff}$  could be calculated:

$$SN_{eff} = (0.0045)(D)(E_p)^{0.33} \# \quad (\text{Eq. 5})\#$$

Where  $SN_{eff}$  = effective structural number

$D$  = total thickness of pavement structure above the subgrade (inches)

$E_p$  = effective modulus of the pavement structure above the subgrade (psi)

To accommodate the large quantity of data, the researchers developed a spreadsheet to calculate  $M_R$ ,  $E_p$ , and  $SN_{eff}$  for each test section. Table 8 presents the statistics of these structural parameters. For most of the sections,  $M_R$  remained fairly constant over the monitoring period. The only exception was observed in Section 041007, where the backcalculated  $M_R$  jumped from 33 ksi in 1994 to 69 ksi in 1995 and decreased to 33 ksi in 1997. This fluctuation could be due to the construction on the section in 1995. In terms of pavement structure, all test sections showed a similar trend in that  $E_p$  and  $SN_{eff}$  remained fairly constant in the 1997, 1999, and 2002 testing. However, researchers observed a decreased  $E_p$  and  $SN_{eff}$  in the last round of testing.

**Table 8. Structural Parameter Statistics for SPS-9A**

Section	Date	M <sub>R</sub> (psi)				E <sub>p</sub> (psi)				SN <sub>eff</sub>
		Average	Maximum	Minimum	COV (%)	Average	Maximum	Minimum	COV (%)	
04B901	1995	28,949	40,648	17,693	19.4	136,723	183,080	98,503	15.0	3.98
04B901	1997	30,949	39,980	21,703	16.4	265,736	366,474	214,224	14.9	5.86
04B901	1999	32,871	41,180	23,327	15.7	274,896	397,821	169,551	19.2	5.87
04B901	2002	37,831	63,421	25,439	27.7	306,204	460,182	156,372	29.2	5.81
04B901	2005	28,529	37,779	19,614	16.3	183,396	311,676	74,500	33.9	4.78
04B902	1995	29,358	32,949	25,105	6.2	134,326	186,140	90,208	17.9	4.00
04B902	1997	32,687	34,782	30,628	4.2	295,456	364,630	240,600	11.5	6.22
04B902	1999	33,542	35,486	30,959	4.5	315,002	393,299	251,270	12.1	6.37
04B902	2002	35,680	43,918	28,849	12.7	332,304	477,059	237,039	20.8	6.24
04B902	2005	29,868	37,235	23,749	12.6	250,433	336,611	182,012	18.1	5.75
04B903	1995	26,580	28,533	24,874	4.1	155,837	230,668	105,480	18.3	4.19
04B903	1997	32,357	41,607	28,577	12.8	286,703	381,018	210,870	13.2	6.33
04B903	1999	31,638	35,479	28,464	5.8	301,070	390,280	234,847	12.6	6.43
04B903	2002	43,805	92,041	29,890	50.4	383,312	631,204	196,096	29.9	6.52
04B903	2005	35,165	53,471	24,310	26.9	279,985	384,813	161,391	23.9	5.91
04B959	1995	19,017	21,774	17,176	6.3	123,133	217,788	68,275	30.5	3.53
04B959	1997	25,928	29,983	21,428	9.2	326,017	462,314	208,958	19.5	6.07
04B959	1999	27,160	31,151	23,189	8.2	315,924	421,827	45,251	24.9	6.10
04B959	2002	25,788	29,404	22,016	8.5	381,757	546,338	246,210	20.6	6.24
04B959	2005	23,765	27,492	20,718	9.0	311,894	436,190	191,329	20.2	5.96
04B960	1995	23,862	25,904	21,126	4.8	171,883	282,444	100,725	24.9	4.03
04B960	1997	30,122	35,505	27,881	6.3	352,891	494,825	279,765	14.8	6.32
04B960	1999	31,379	36,306	29,211	5.2	353,936	498,019	45,357	23.2	6.41
04B960	2002	30,024	33,951	27,723	4.6	413,589	590,113	323,200	15.7	6.61
04B960	2005	29,167	34,731	25,585	7.0	356,083	508,556	248,675	18.0	6.26
04B961	1995	28,151	30,832	24,254	5.5	158,711	236,806	99,114	24.3	3.96
04B961	1997	33,420	36,819	30,685	5.1	372,434	460,651	276,907	13.0	6.44
04B961	1999	34,192	37,360	30,934	4.8	387,084	482,755	287,473	13.6	6.52
04B961	2002	33,709	36,783	31,509	4.7	422,313	528,367	316,203	14.9	6.60
04B961	2005	32,191	38,099	28,905	8.1	374,253	454,893	290,402	13.0	6.40
04B964	1995	38,767	47,576	28,941	14.4	184,452	323,261	108,978	29.0	4.10
04B964	1997	41,652	49,051	30,434	11.4	325,854	425,091	219,385	16.7	6.03
04B964	1999	43,940	52,980	32,478	12.3	319,282	424,569	215,871	18.1	5.99
04B964	2002	46,528	59,964	33,516	14.4	363,137	499,699	251,992	19.8	6.25
04B964	2005	41,183	49,657	29,079	13.7	347,947	455,412	197,200	17.9	6.22
041007	1989	49,092	65,536	36,758	14.4	133,433	194,227	67,490	28.5	3.48
041007	1991	38,798	48,721	30,569	10.0	164,005	263,434	78,824	30.5	3.79
041007	1994	33,301	40,727	26,524	9.9	186,302	289,728	81,070	34.9	3.86
041007	1995	69,973	86,868	55,787	11.9	116,089	178,055	77,353	25.3	4.30
041007	1997	33,205	36,522	27,632	6.1	338,247	461,604	184,745	20.3	6.20
041007	1999	34,584	38,738	28,995	6.1	399,774	529,702	204,192	20.2	6.64
041007	2002	35,338	56,764	26,784	16.6	353,617	537,917	149,727	28.5	5.93
041007	2005	31,516	61,815	24,346	18.5	239,315	461,379	94,113	34.2	5.26

## BACKCALCULATION USING EVERCALC SOFTWARE

The FWD data were also processed through the backcalculation software Evercalc developed by Washington State Department of Transportation. One set of FWD data at each station was selected for backcalculation using the representative thickness of each test section obtained from the LTPP database to determine  $M_R$  of each layer. Table 9 shows the seed value and modulus range used for backcalculation. The pavement structure was first assumed as a four-layer system for analysis: AC, aggregate base (AB), subgrade, and bedrock. However, after running several initial analyses, the researchers found that the base layer was not producing reasonable moduli values. Consequently, instead of calculating each individual layer moduli, the base layer was combined into the subgrade layer for consideration, and the backcalculation analysis was repeated. The results of this approach produced more reasonable moduli values.

**Table 9. Backcalculation Seed Value and Modulus Range**

<b>Layer Description</b>	<b>Seed Modulus (ksi)</b>	<b>Poisson's Ratio</b>	<b>Minimum Modulus (ksi)</b>	<b>Maximum Modulus (ksi)</b>
AC	400	0.35	100	2100
AB	25	0.3	10	150
Subgrade	15	0.4	5	50

Table 10 provides the statistics of backcalculated moduli for the test sections. A similar pavement response was observed on the three LTPP test sections (04B901, 04B902, and 04B903). A rapid increment of the AC moduli was observed in the second round of testing (1997). The AC moduli dropped significantly in 2002. In general, Sections 04B902 and 04B903 (SP-1) showed a higher AC moduli value compared to Section 04B901 (agency standard mix). No significant difference was found between Section 04B902 (PG 76-10) and Section 04B903 (PG 70-10). All three SMA sections (04B959, 04B960, and 04B961) showed superior AC moduli among the eight test sections. Section 04B964 (ARAC) and Section 041007 (SP-3) showed the lowest AC moduli values.

**Table 10. Backcalculation Moduli Statistics for SPS-9A Test Sections**

<b>Section</b>	<b>Date</b>	<b>Backcalculated AC Modulus (ksi)</b>	<b>Backcalculated Subgrade Modulus (ksi)</b>	<b>Root-Mean Square Error (%)</b>
04B901	1995	389.7	25.7	6.07
04B901	1997	693.5	33.5	5
04B901	1999	729.9	35.8	3.72
04B901	2002	340.8	39.4	8.48
04B901	2005	321.7	29.1	3.12
04B902	1995	320.3	23.7	8.2
04B902	1997	793.8	36.8	5.78
04B902	1999	831.8	36.8	5.58
04B902	2002	428.1	38.5	9.9
04B902	2005	468.8	31.1	6.62
04B903	1995	487.8	22.5	4.93
04B903	1997	774	34.9	5.18
04B903	1999	806.4	32.8	4.99
04B903	2002	554.5	42.5	8.17
04B903	2005	554.2	35.4	6.23
04B959	1995	509.4	15.9	2.63
04B959	1997	1257.7	25.1	1.34
04B959	1999	1469.8	27.5	1.93
04B959	2002	833.1	24.2	1.78
04B959	2005	1112.4	22.5	1.77
04B960	1995	303.5	19.4	8.09
04B960	1997	1730	32.5	3.33
04B960	1999	1514.6	33.5	3.8
04B960	2002	723	30.5	5.14
04B960	2005	1309.4	29.8	2.85
04B961	1995	505.4	24	2.23
04B961	1997	1593.7	35.9	2.52
04B961	1999	1563.6	35.5	2.28
04B961	2002	1343.8	36.3	3.06
04B961	2005	1273.4	34.9	2.48
04B964	1995	448.8	31.1	18.87
04B964	1997	703.5	48.2	11.27
04B964	1999	590	48.3	12.47
04B964	2002	353.5	50	18.84
04B964	2005	626.3	45.5	10.25
041007	1989	373.8	30.1	10.1
041007	1991	304.1	29.4	3.66
041007	1994	412.2	24.6	2.17
041007	1995	244.5	24.2	7.18
041007	1997	906.2	32.9	2.71
041007	1999	845.9	34.2	3.43
041007	2002	457.7	34.1	4.39
041007	2005	409.8	30.1	2.17

In general, backcalculated AC modulus decreased as the pavement aged (Figure 10). In some cases the AC modulus increased with time, which could be due to aging of the asphalt binder. The decrease in AC moduli value is probably due to the appearance of distress and the resulting weakening in overall pavement strength.

Figure 11 shows the backcalculated subgrade modulus values. The variation in the Evercalc backcalculated subgrade modulus within each section is similar to the previous backcalculated subgrade modulus using the American Association of State Highway and Transportation Officials (AASHTO) procedure except Section 041007. In general, uniform subgrade modulus was observed at the test site during the test period. The average backcalculated subgrade modulus of all sections is 32 ksi. The highest coefficient of variation (COV) of the subgrade modulus was 21 percent in Section 04B903; the lowest COV was 14 percent in Section 041007.

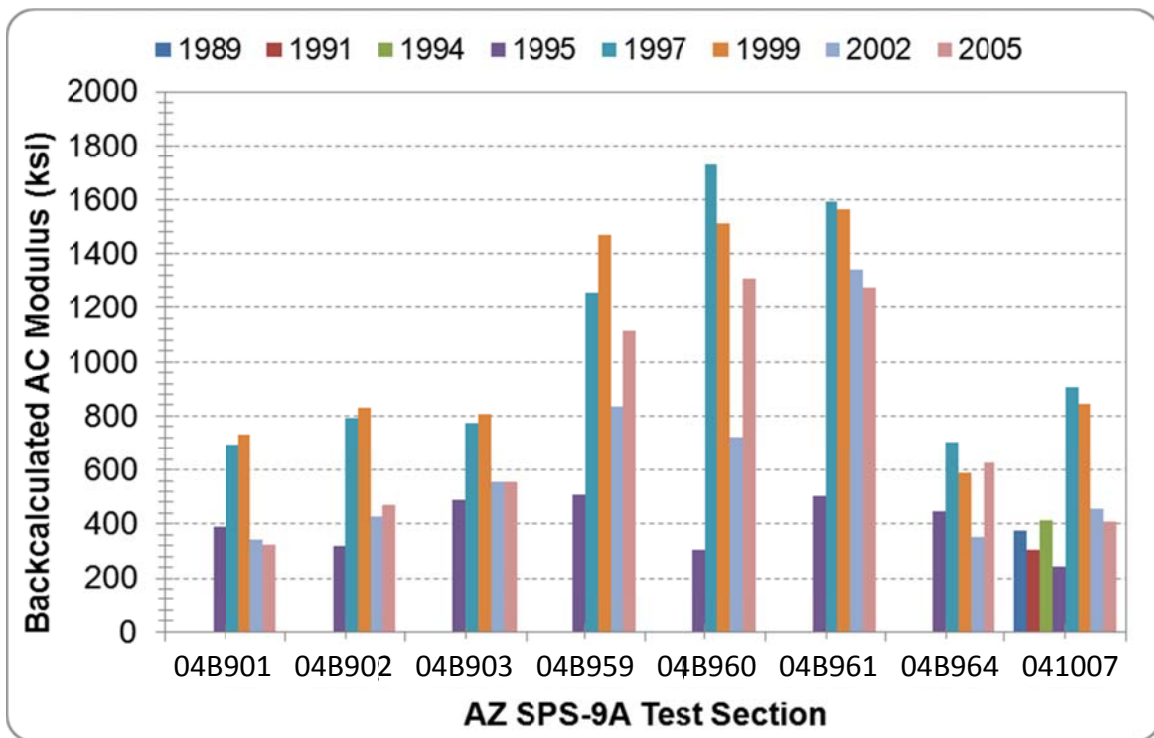


Figure 10. Backcalculated AC Modulus by Test Section

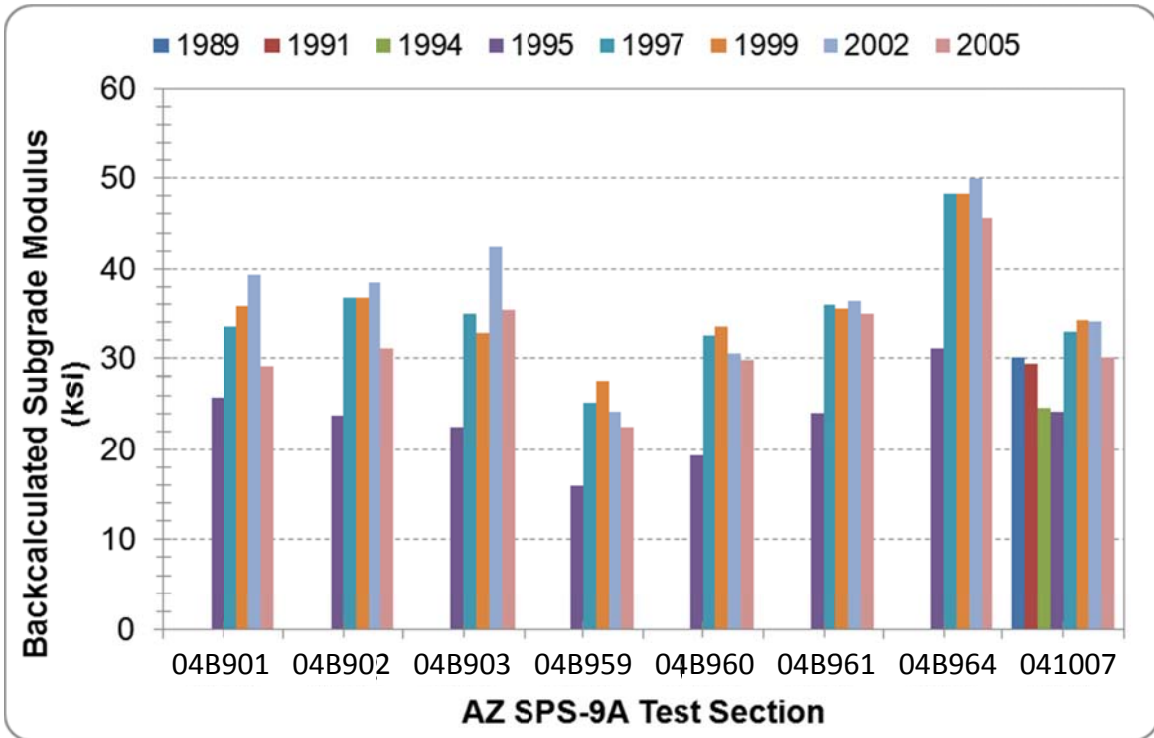


Figure 11. Backcalculated  $M_R$  by Test Section

#### KEY FINDINGS FROM THE SPS-9A DEFLECTION ANALYSIS

The deflection at the center plate shows an improvement in pavement strength between testing conducted in 1995 and 1997 as a result of adding the structural layer in 1995 after the first round of testing was completed. All of the sections remained structurally sound during the 1997, 1999, and 2002 testing. The researchers observed a decline in pavement structure in the last round of testing in 2005, mainly due to the weakening in the AC layer, since the subgrade didn't change significantly over time.

The  $M_R$ ,  $E_p$ , and  $SN_{eff}$  results after using the *AASHTO Guide for Design of Pavement Structures* (1993) procedure follow:

- The average  $E_p$  showed an increasing trend in the second, third, and fourth round of testing and decreased in the last round of testing. These results can be explained by age hardening of the AC layer. A decrease of  $E_p$  was observed in the last round of testing because significant pavement distresses developed.
- After the 1995 construction, the average backcalculated  $SN_{eff}$  did not change significantly within each section over the monitoring period.

The results of  $M_R$  and the AC moduli after using the industrial standard backcalculation software Evercalc are summarized below:

- After construction in 1995, little variation in the AC moduli was observed in most sections. The first significant drop was observed in 2002 in all sections, however, the AC moduli bounced back in the 2005 testing. A similar trend was observed among the three core LTPP test sections. The Superpave mix design sections showed higher AC moduli values compared to the agency standard mix section. No significant difference was found between the PG 76-10 and PG 70-10 sections. The three SMA sections showed the highest AC moduli value among all test sections.
- The trend of the Evercalc backcalculated subgrade moduli was similar to the trend observed in the subgrade moduli using the AASHTO procedure. In general, uniform subgrade modulus was observed at the test site during the test period. The average backcalculated subgrade modulus of all sections was 32 ksi. The COV of subgrade modulus within each test section ranged from 14 percent to 21 percent.



## CHAPTER 3. SPS-9A DISTRESS ANALYSIS

This chapter includes analyses and results from evaluating distress data collected from the SPS-9A site using LTPP manual survey techniques (Miller and Bellinger 2003). Surface distress provides powerful information about the nature and extent of pavement deterioration, which can be used to quantify performance trends as well as to investigate how design features affect service life.

All of the flexible SPS-9A test sections were constructed consecutively and exposed to the same traffic-loading, climate, and subgrade conditions, allowing for direct comparisons between layer configurations and design features without the confounding effects introduced by different in situ conditions.

### AC DISTRESS TYPES

Surface deterioration is composed of multiple distress types. The raw distress data for each section are not included in this report but are available for download from LTPP Products Online (<http://www.infopave.com/Data/StandardDataRelease/>). Distress type definitions follow (Huang 1993):

- **Fatigue cracking:** A series of interconnecting cracks caused by repeated traffic loading. Cracking initiates at the bottom of the asphalt layer where tensile stress is the highest under the wheel load. With repeated loading, the cracks propagate to the surface.
- **Longitudinal wheelpath (WP) cracking:** Cracking parallel to the centerline occurring in the WP. This cracking can be the early stages of fatigue cracking or can initiate from construction-related issues such as paving seams and segregation of the mix during paving. In the latter case, cracking is typically very straight (no meandering).
- **Longitudinal non-wheelpath (NWP) cracking:** Cracking parallel to the centerline occurring outside the WP. This cracking is not load-related and can initiate from paving seams or where segregation issues occurred during paving. Cracking can also be caused by tensile forces experienced during temperature changes. Pavements with oxidized or hardened asphalt are more prone to this type of cracking.
- **Transverse cracking:** Cracking that is predominantly perpendicular to the pavement centerline. Cracking starts from tensile forces experienced during temperature changes. Pavements with oxidized or hardened asphalt are more prone to this type of cracking.
- **Block cracking:** Cracking that forms a block pattern and divides the surface into approximately rectangular pieces. Cracking initiates from tensile forces experienced during temperature changes. This distress type indicates that the AC has significantly oxidized or hardened.
- **Raveling:** Wearing away of the surface caused by dislodging of aggregate particles and loss of asphalt binder. Raveling is caused by moisture stripping and asphalt hardening.

- Bleeding: Excessive bituminous binder on the surface that can lead to loss of surface texture or a shiny, glass-like, reflective surface. Bleeding is a result of high asphalt content or low air void content in the mix.
- Rutting: A surface depression in the WPs. Rutting can result from consolidation or lateral movement of material due to traffic loads. It can also signify plastic movement of the asphalt mix because of inadequate compaction, excessive asphalt, or a binder that is too soft given the climatic conditions.

These distress types can be grouped into two general categories based on cause of failure mechanism: structural or environmental factors. Table 11 summarizes the flexible pavement distress types and their associated failure mechanisms.

**Table 11. Flexible Pavement Distress Types and Failure Mechanisms**

Distress Type	Failure Mechanism	
	Traffic/Load Related	Climate/Materials Related
Fatigue cracking	X	
Longitudinal WP cracking	X	
Longitudinal NWP cracking		X
Transverse cracking		X
Block cracking		X
Raveling		X
Bleeding		X
Rutting	X	X

## RESEARCH APPROACH

Investigators began this analysis with a cursory review of all distress data collected at each test section to identify suspect or inconsistent information. Team members used photos and distress maps to verify quantities reported in the database. Because of the subjective nature of the data collection technique (raters must select distress type and severity based on a set of rules), variation is expected in distress data. The SPS-9A data set was well within the acceptable range of variability.

Distress data are reported at three severity levels: low, moderate, and high. Inconsistencies between severity levels within a distress type create one of the largest sources of variability in distress data (Rada et al. 1999). In addition, conducting analyses on three separate severity levels for each distress type becomes increasingly complex with results that are difficult to interpret. To reduce variability and to

consolidate the information for analyses, the researchers summed the quantities from the three severity levels into one composite value.

As shown in Table 11, pavement deterioration (when not directly attributable to mix problems or construction deficiencies) can be attributed to structural or environmental factors. Structural factors are the result of traffic loading relative to the structural capacity of the pavement section. Environmental factors represent the influence of climate on pavement deterioration. Therefore, structural and environmental indices were developed to focus the analyses on overall structural and environmental damage, which are more consistent and provide a better avenue for comparison, rather than on individual types of distress, which vary from section to section and year to year.

The structural damage index consists of those distresses generally manifesting from the portion of the pavement that experiences loading (i.e., WPs). Therefore, the structural damage index was presented as the percentage of WP damage and included fatigue and longitudinal WP cracking. To normalize fatigue and longitudinal cracking, the structural damage index took the form of the following expression:

$$S = \frac{F + 1ft \times C_{lwp}}{2W_{wp} L_s} \# \quad (\text{Eq. 6})$$

Where  $S$  = structural damage index

$F$  = area of fatigue (ft<sup>2</sup>)

$C_{lwp}$  = length of longitudinal WP cracking (ft)

$W_{wp}$  = width of WP = 3.28 (ft)

$L_s$  = length of test section (ft)

The environmental damage index is a composite of distresses that generally result from climatic effects. The entire pavement surface is subject to environmental distress; therefore, the environmental damage index was characterized as the percentage of total pavement area damaged. Typically, transverse cracking, longitudinal cracking (outside of the WPs), and block cracking are specific to environmental damage. To normalize the environmental distress for the total area, the environmental damage index was expressed as:

$$E = \frac{B}{A_{tot}} + \frac{C_{nwp}}{L_s} + \frac{C_t}{L_s} \# \quad (\text{Eq. 7})$$

Where  $E$  = environmental damage index  
 $B$  = area of block cracking (ft<sup>2</sup>)  
 $C_{nwp}$  = length of NWP cracking (ft)  
 $C_t$  = length of transverse cracking (ft)  
 $A_{tot}$  = total area of test section (ft<sup>2</sup>)  
 $L_s$  = length of test section (ft)

Although the structural and environmental distress factors clearly affected the SPS-9A project's structural and functional service life, rutting, patching, and other surface defects (such as potholes, bleeding, and raveling) also affected performance. Rutting data reported in this study were generated using a 6 ft straightedge reference (Simpson 2001).

Replicate data were not collected for the SPS-9A project. Therefore, standard statistical comparisons (i.e.,  $t$  tests) to determine the significance of findings could not be conducted. Instead, the evaluation consisted of graphical comparisons between test sections from data collected at the same points in time.

#### **OVERALL PERFORMANCE TREND OBSERVATIONS**

While gathering pavement distress data, researchers became aware of a few significant trends affecting the overall pavement performance of the project. These observations were clearly driving issues for this project and were intrinsically important pieces of the distress performance.

Before receiving the experimental AC overlays, each section received the same rehabilitation treatment and existing AC was milled. Manual distress surveys were performed on each section after milling, but before the experimental layers were added. These surveys showed similar conditions throughout all the sections.

No global preventive maintenance or rehabilitation was performed on any of the test sections. Sections 04B961 and 04B964 exhibited raveling in the 2005 and 2002 surveys, respectively. Sections 04B902 and 041007 exhibited significant pumping; Sections 04B903 and 04B959 experienced minimal pumping.

Figure 12 shows the structural damage trends for each section. The performance trends are relatively consistent and within the expected range of variation. All sections (except 04B959 and 04B961) showed a rapid accumulation of structurally related distresses approximately 10 years after construction.

The Marshall mix (Section 04B901) contained a smaller percentage of asphalt binder than the Superpave mixes (Sections 04B902 and 04B903). Higher asphalt binder contents typically produce better resistance to fatigue cracking; however, all three sections accumulated similar amounts of fatigue cracking. Compared to the rest of the SPS-9A project, Section 04B959 (SMA polymer with ACFC) and Section 04B961 (SMA cellulose) exhibited significantly smaller amounts of structural damage accumulation.

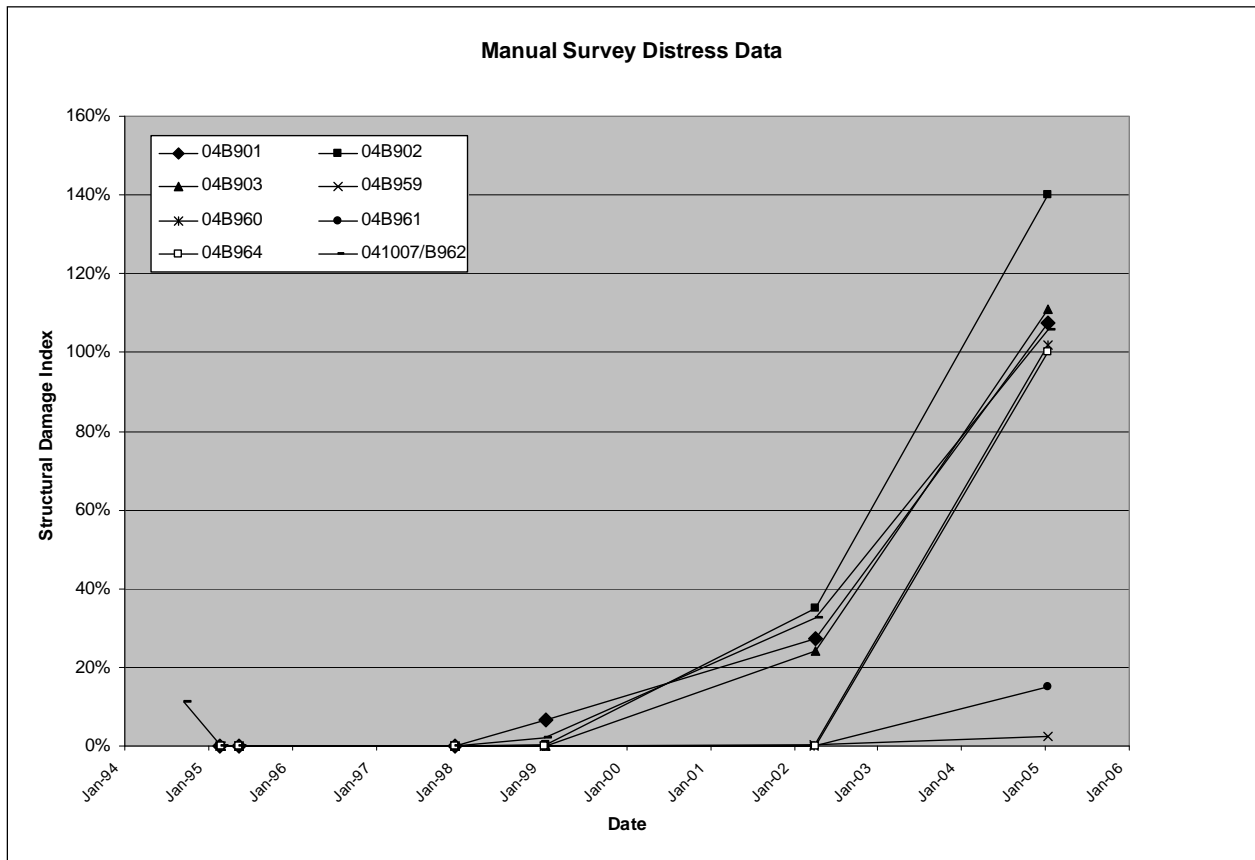


**Figure 12. Structural Damage Trends for SPS-9A Test Sections**

Figure 13 shows the overall environmental damage trends for each section. The performance trends are relatively consistent and within the expected range of variation.

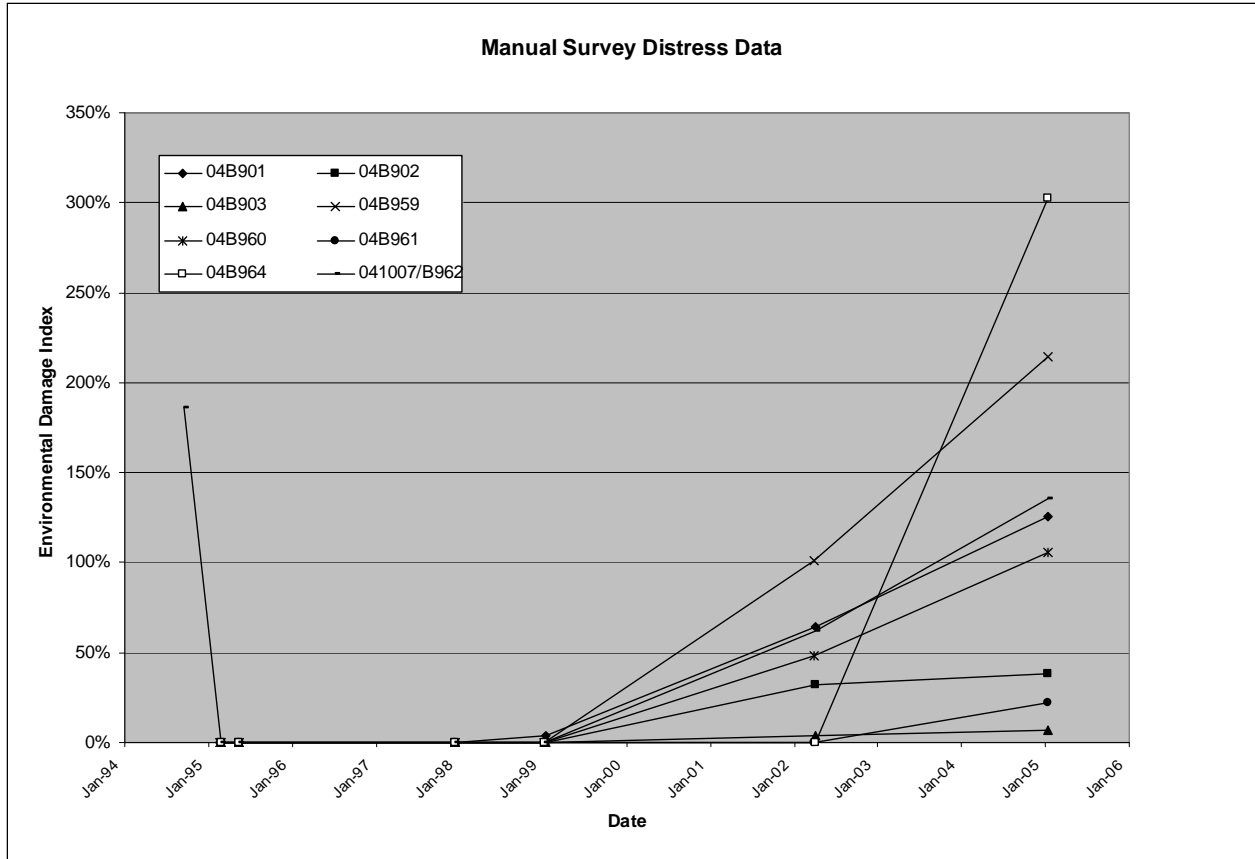
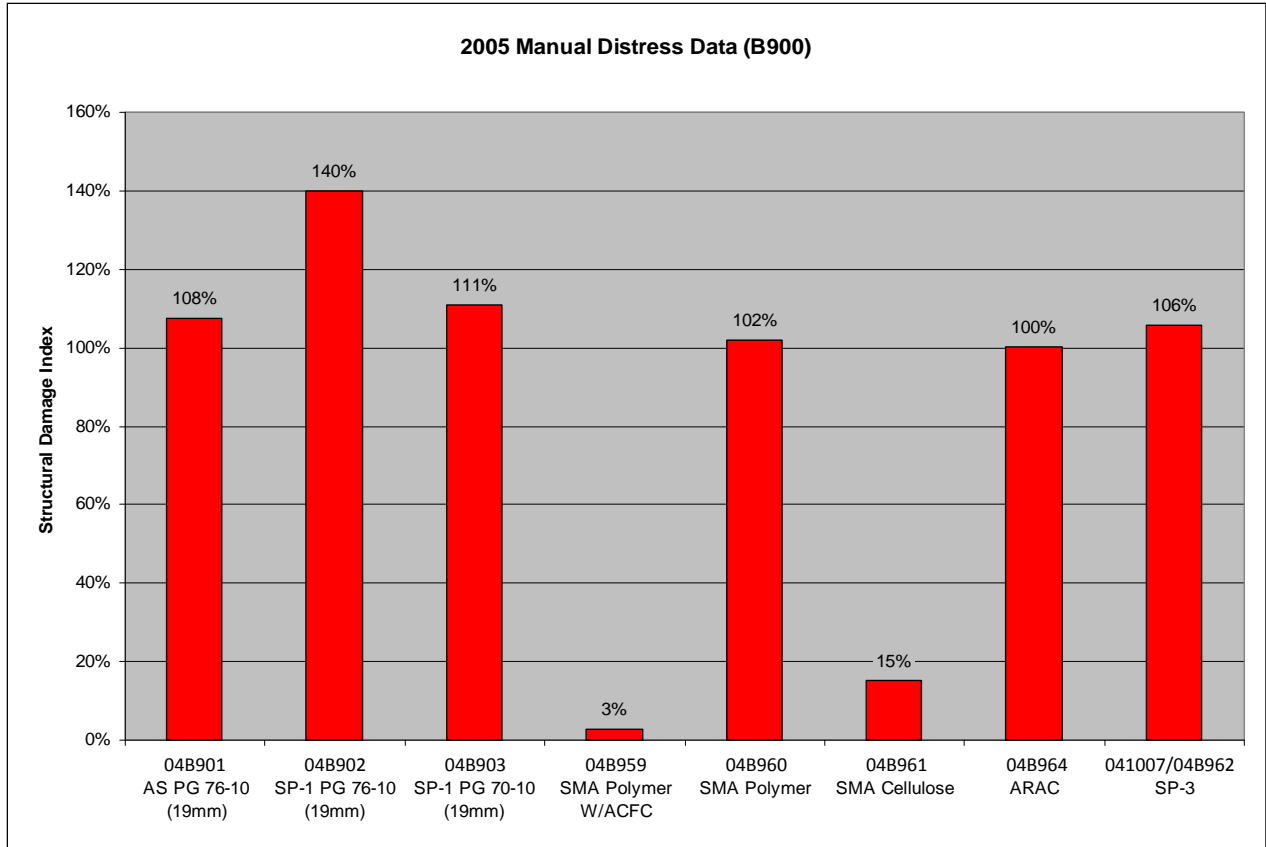


Figure 13. Environmental Damage Trends for SPS-9A Test Sections

### Performance Comparisons

In-depth analyses and comparisons were conducted for all of the SPS-9A test sections. Figure 14 summarizes the structural damage index and pavement structure for each section; Figure 15 summarizes the environmental damage index and pavement structure. Both damage indices reported are based on the data collected in January 2005 (just before going out of study).



**Figure 14. Structural Damage Index and Pavement Structure Summary**

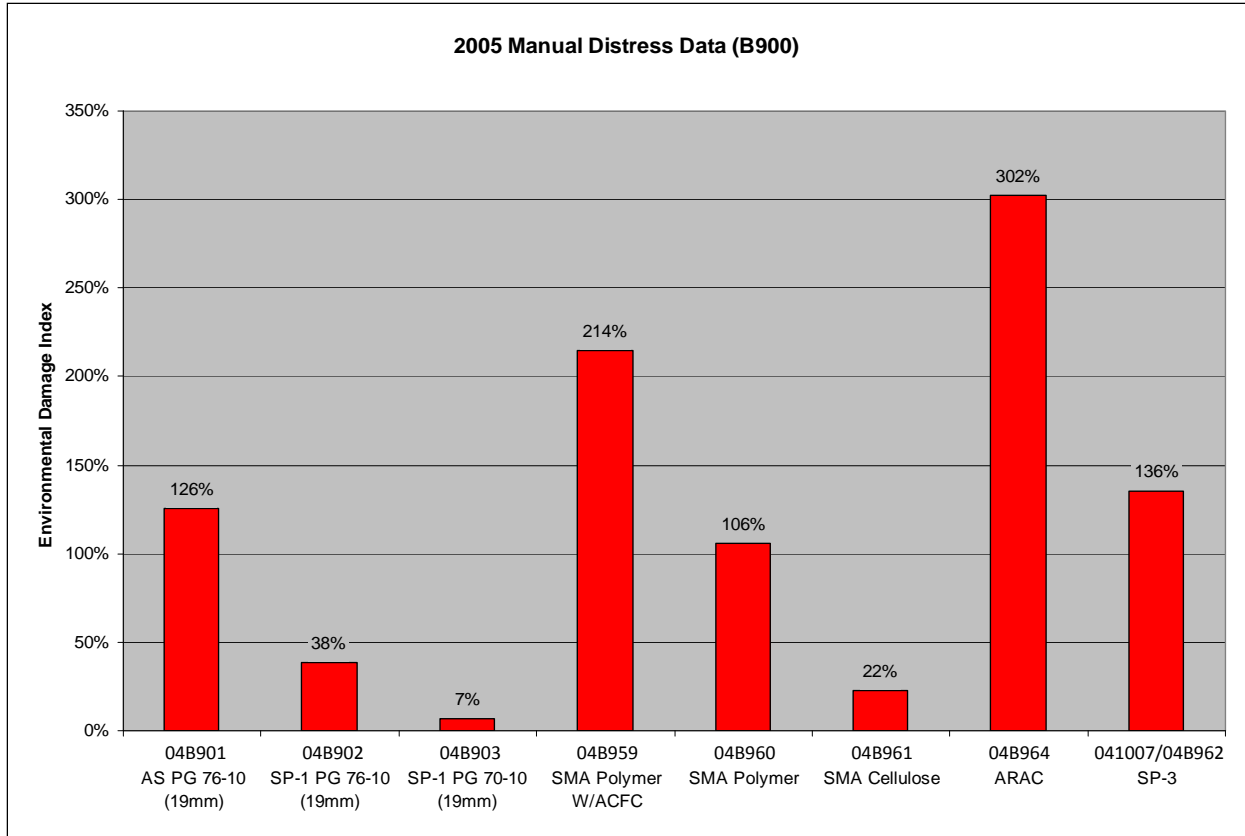


**Figure 15. Environmental Damage Index and Pavement Structure Summary**

Figure 16 summarizes the rutting and pavement structure for each section. Significant variation in rutting performance between the sections did not exist. All sections exhibited less than 7 mm of rutting after over seven years in service, which is well below the level required to trigger improvements in most pavement management systems. Therefore, rutting was not the driving factor in the overall condition of the pavement.

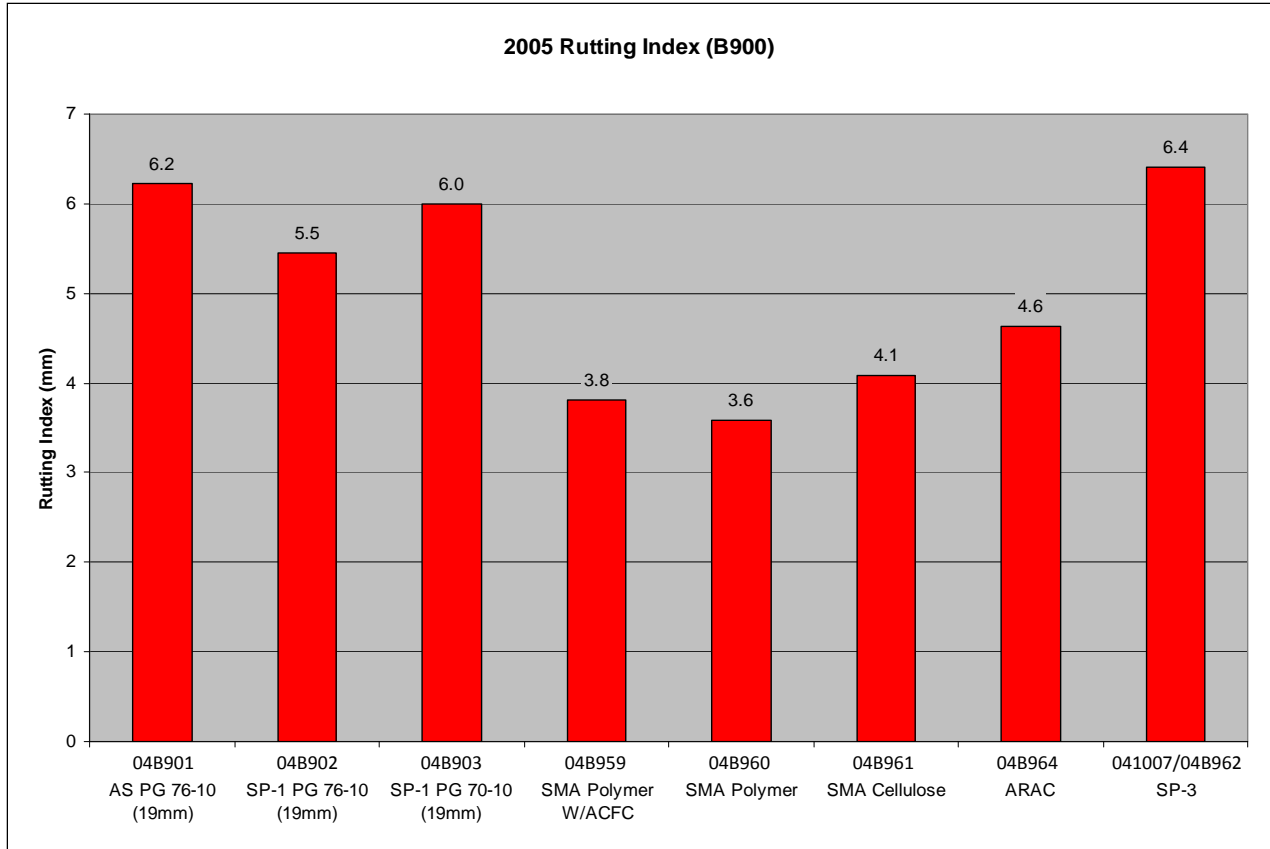


**Figure 16. Rutting Index and Pavement Structure Summary**

Following is a synopsis of the findings and performance of each section, including structural deterioration, environmental deterioration, rutting, and other unique circumstances.

*Section 04B901 (Standard Agency Mix, Marshall 75, PG 76-10)*

This section exhibited average cracking performance, both structurally and environmentally. The structural damage index was 108 percent. Five of eight test sections experienced similar quantities of structural damage. The environmental damage index was 126 percent. Three of eight test sections experienced similar quantities of structural damage. The rate of structural and environmental deterioration increased from 2002 to 2005.

*Section 04B902 (SP-1, PG 76-10)*

This section exhibited the most structural damage of all the test sections; however it performed very well against environmental damage. The structural damage index was 140 percent, while most sections experienced quantities near 100 percent. The environmental damage index was 38 percent—much

lower than the majority of the test sections, which experienced quantities from 100 percent to 300 percent. Section 04B902 also exhibited the highest amount of pumping among the test sections. The rate of structural deterioration increased from 2002 to 2005.

*Section 04B903 (SP-1, AC-40 [PG 70-10])*

Structural deterioration was average in this section, but the environmental deterioration was well below the average for the SPS-9A project. In fact, Section 04B903 exhibited the highest resistance to environmental damage. The rate of structural deterioration increased from 2002 to 2005.

*Section 04B959 (SMA Polymer with ACFC)*

This section exhibited the highest resistance against structural damage for the SPS-9A project. After 10 years, the structural damage index was at 3 percent, while most sections had a structural damage index over 100 percent. However, this section also exhibited the second largest amount of environmental damage of the entire SPS-9A project as a result of NWP longitudinal cracking along the edge of the lanes throughout the entire section. The rate of environmental deterioration increased from 2002 to 2005.

*Section 04B960 (SMA Polymer)*

Like Section 04B901, this section exhibited average cracking performance, both structurally and environmentally. The structural damage index was 102 percent. Five of eight test sections experienced similar quantities of structural damage. The environmental damage index was 106 percent. Three of eight test sections experienced similar quantities of structural damage. The rate of structural and environmental deterioration increased from 2002 to 2005.

*Section 04B961 (SMA Cellulose)*

This section was the best-performing pavement in the entire SPS-9A project. It was significantly better at resisting structural and environmental damage throughout the duration of its life when compared to the other test sections. The environmental and structural damage indices were each approximately 20 percent, which was significantly lower than the majority of the other test sections. Sections 04B961 and 04B964 experienced the highest amount of pavement raveling.

*Section 041007/04B962 (SP-3)*

Like Sections 04B901 and 04B960, this section exhibited average cracking performance, both structurally and environmentally. The structural damage index was 106 percent. Five of eight test sections experienced similar quantities of structural damage. The environmental damage index was 136 percent. Three of eight test sections experienced similar quantities of structural damage. Like Section 04B902, this section exhibited a significant amount of pumping. The rate of structural and environmental deterioration increased from 2002 to 2005.

### *Section 04B964 (ARAC)*

This section performed average against structural damage, but accumulated the highest amount of environmental damage. The structural damage index was 100 percent. Five of eight test sections experienced similar quantities of structural damage. However, the environmental damage index was 302 percent, which was significantly higher than all the other test sections. Sections 04B964 and 04B961 experienced the highest amount of pavement raveling.

### **KEY FINDINGS FROM THE SPS-9A DISTRESS ANALYSIS**

The distress data captured at the SPS-9A project provide valuable insight into pavement performance, design, management, and construction. Highlights from the SPS-9A distress analysis follow:

- Most every section (except Sections 04B959 and 04B961) showed significant growth in fatigue and longitudinal cracking 10 years after construction.
- Construction quality can play a major role in performance. The construction observations documented in the LTPP construction report were limited to Sections 04B901, 04B902, and 04B903. However, the report showed that all three sections were free of any construction issues.
- Half the sections (04B901, 04B959, 04B960, and 041007/04B962) had reasonable patterns of environmental distress growth with a clear increase in magnitude approximately 10 years after construction. Section 04B964 had little environmental distress growth for seven years but it rapidly increased after 10 years.
- For the SP-1 mix designs (Sections 04B902 and 04B903), the PG 70-10 binder (Section 04B903) performed significantly better structurally and environmentally than the PG 76-10 binder (Section 04B902). It also performed significantly better than the standard agency mix at resisting environmental deterioration.
- SMA with cellulose fibers was, by far, the best pavement mix at resisting both structural and environmental deterioration.
- All sections performed well with regard to rut resistance. Rutting would not have triggered a rehabilitation event for any section.
- With no replicate sections, there is limited ability to assess potential variability independent of actual performance.
- Three sections (Sections 04B959, 04B902, and 041007/04B962) received patching at some point.



## CHAPTER 4. SPS-9A ROUGHNESS ANALYSIS

This chapter characterizes the surface roughness of these sections throughout their service life and links the observations to records of pavement distress and its development. Investigators collected road profile measurements on this site about once per year starting with the winter after the site was opened to traffic. This study analyzed the profiles in detail by calculating their roughness values, examining the spatial distribution of roughness within them, viewing them with post-processing filters, and examining their spectral properties. These analyses provided details about the roughness characteristics of the road and provided a basis for quantifying and explaining the changes in roughness with time.

### PROFILE DATA SYNCHRONIZATION

Profile data were collected from the entire SPS-9A site on eight dates, from January 29, 1997, through December 17, 2004 (Table 12). Raw profile data were available for all visits. Each visit produced a minimum of five repeat profile measurements.

**Table 12. Profile Measurement Visits of the SPS-9A Site**

Visit	Date	Repeats by Section							
		04B901	04B902	04B903	04B959	04B960	04B961	04B962	04B964
01	Jan. 29, 1997	7	7	7	7	7	7	7	7
02	Feb. 2, 1997	—	—	—	—	—	—	9	9
03	Dec. 5, 1997	7	7	7	7	7	7	7	7
04	Dec. 7, 1998	5	7	5	5	5	5	7	7
05	Nov. 10, 1999	7	7	7	7	7	7	7	7
06	Nov. 12, 2001	7	9	7	9	7	9	7	9
07	Feb. 09, 2004	9	9	9	9	9	9	9	9
08	Dec. 17, 2004	9	9	9	9	9	9	9	9

In visit 01, all eight sections were covered together in each profile. Visit 02 only covered Sections 04B962 and 04B964. Visit 03 covered Sections 04B962 and 04B964 together in one set of passes, and all of the other sections together in another. Each section was measured individually in visits 04 through 08.

Researchers used the raw data to synchronize all of the profiles to each other through their entire history. Three clues were available for this purpose: (1) the site layout from the construction report, (2) event markers in the raw profiles from the start and end of each section, and (3) automated searching for the longitudinal offset between repeat measurements.

## **DATA EXTRACTION**

Researchers extracted profiles of individual test sections directly from the raw measurements for two reasons: First, profiles were collected in visits 01 through 06 at a 0.98-inch sample interval and in visits 07 and 08 at about a 0.77-inch sample interval. These data appeared in the database after the application of an 11.8-inch moving average and decimation to a sample interval of 5.91 inches. The raw data contained the more detailed profiles. Second, this study depended on consistency of the profile starting and ending points with the construction layout and consistency of the section limits with time. In particular, a previous quality check revealed some profiles were shifted (Evans and Eltahan 2000).

## **CROSS CORRELATION**

Searching for the longitudinal offset between repeat profile measurements that provides the best agreement between them is a helpful way to refine their synchronization. This can be done by inspecting filtered profile plots, but it is very time-consuming. Visual assessment is also somewhat subjective when two profiles do not agree well, which is often the case when measurements are made several years apart. In this study, investigators used an automated procedure rather than visual inspection to find the longitudinal offset between measurements.

In this procedure, which is based on a customized version of cross correlation (Karamihas 2004), a basis measurement is designated that is considered to have the correct longitudinal positioning. A candidate profile is then searched for the longitudinal offset that provides the highest cross correlation to the basis measurement. A high level of cross correlation requires a good match of profile shape, the location of isolated rough spots, and overall roughness level. Therefore, the correlation level is often only high when the two measurements are synchronized. When the optimal offset is found, a profile is extracted from the candidate measurement with the proper overall length and endpoint positions. For the remainder of this discussion, this procedure will be referred to as automated synchronization.

For this application, investigators performed cross correlation after the International Roughness Index (IRI) filter was applied to the profiles rather than using the unfiltered profiles, which helped assign the proper weighting to relevant profile features. In particular, it increased the weighting of short-wavelength roughness that may be linked to pavement distress. This enhanced the effectiveness of the automated synchronization procedure. The long-wavelength content within the IRI output helped ensure that the longitudinal positioning was nearly correct, and the short-wavelength content was able to leverage profile features at isolated rough spots to fine-tune the positioning.

## **SYNCHRONIZATION**

To extract profiles of individual test sections from the raw measurements, investigators:

1. Established a basis measurement for each section from visit 08. The first repeat measurement was used for this purpose. All of the sections were 500 ft long.
2. Automatically synchronized the other eight repeats from visit 08 to the basis set.
3. Automatically synchronized the measurements from the previous visit to the current basis set.
4. Designated the previous visit as the current visit.
5. Replaced the basis set with a new set of synchronized measurements from the first repeat of the current visit.
6. Repeated steps 3 through 5 until visit 01 was complete.

## **DATA QUALITY SCREENING**

Investigators performed data quality screening to select five repeat profile measurements from each visit of each section. Among the group of available runs, investigators selected the five measurements that exhibited the best agreement with each other. In this case, agreement between any two profile measurements was judged by cross-correlating them after applying the IRI filter (Karamihas 2004). In this method, the IRI filter is applied to the profiles; then the output signals are compared rather than the overall index. High correlation by this method requires that the overall roughness as well as the details of the profile shape that affect the IRI agree. The IRI filter was applied before correlation in this case for several reasons:

- Direct correlation of unfiltered profiles places a premium on very long-wavelength content, but ignores much of the contribution of short-wavelength content.
- Correlation of IRI filter output emphasizes profile features in (approximate) proportion to their effect on the overall roughness.
- Correlation of IRI filter output provides a good trade-off between emphasizing localized rough features at distressed areas in the pavement and placing too much weight on the very short-duration, narrow features (spikes) that are not likely to agree between measurements because the IRI filter amplifies short-wavelength content, but attenuates macrotecture, megatecture, and spikes.
- A relationship has been demonstrated between the cross-correlation level of IRI filter output and the expected agreement in overall IRI (Karamihas 2004).

Note: This method was performed with a special provision for correcting modest longitudinal distance measurement errors.

Each comparison between profiles produced a single value that summarized their level of agreement. When nine repeat profile measurements were available, they produced 36 correlation values. Any subgroup of five measurements could be summarized by averaging the relevant 10 correlation values. Researchers selected the subgroup that produced the highest average and excluded the other repeats from most of the analyses discussed in the remainder of this report. Since the number of available profiles ranged from six to nine, the number of measurements that were excluded ranged from one to four. Tables 13 through 20 list the selected repeats for each visit of each section and the composite correlation level produced by them.

**Table 13. Selected Repeats of Section 04B901**

<b>Visit</b>	<b>Repeat Numbers</b>					<b>Composite Correlation</b>
01	1	2	3	5	6	0.901
03	1	3	4	5	7	0.898
04	1	2	3	4	5	0.916
05	2	4	5	6	7	0.912
06	2	3	4	6	7	0.870
07	1	3	5	7	9	0.659
08	2	3	5	7	8	0.722

**Table 14. Selected Repeats of Section 04B902**

<b>Visit</b>	<b>Repeat Numbers</b>					<b>Composite Correlation</b>
01	2	3	4	5	7	0.935
03	1	3	4	5	7	0.896
04	1	2	4	5	6	0.931
05	2	3	4	5	6	0.871
06	5	6	7	8	9	0.827
07	3	6	7	8	9	0.639
08	1	5	7	8	9	0.768

**Table 15. Selected Repeats of Section 04B903**

<b>Visit</b>	<b>Repeat Numbers</b>					<b>Composite Correlation</b>
01	2	3	5	6	7	0.929
03	1	2	4	6	7	0.914
04	1	2	3	4	5	0.918
05	3	4	5	6	7	0.943
06	1	3	4	6	7	0.894
07	1	3	5	6	7	0.853
08	1	2	3	8	9	0.588

**Table 16. Selected Repeats of Section 04B959**

<b>Visit</b>	<b>Repeat Numbers</b>					<b>Composite Correlation</b>
01	1	3	4	6	7	0.932
03	1	2	4	5	7	0.923
04	1	2	3	4	5	0.921
05	2	3	4	5	6	0.922
06	2	5	7	8	9	0.944
07	1	3	5	6	7	0.905
08	3	5	6	8	9	0.870

**Table 17. Selected Repeats of Section 04B960**

<b>Visit</b>	<b>Repeat Numbers</b>					<b>Composite Correlation</b>
01	1	2	3	5	7	0.925
03	1	2	4	6	7	0.915
04	1	2	3	4	5	0.903
05	1	2	3	4	6	0.924
06	1	2	3	4	7	0.949
07	1	2	3	4	5	0.853
08	5	6	7	8	9	0.864

**Table 18. Selected Repeats of Section 04B961**

<b>Visit</b>	<b>Repeat Numbers</b>					<b>Composite Correlation</b>
01	1	2	3	4	7	0.943
03	2	4	5	6	7	0.948
04	1	2	3	4	5	0.915
05	1	2	4	5	7	0.942
06	1	2	3	4	6	0.953
07	2	3	5	6	9	0.901
08	1	6	7	8	9	0.826

**Table 19. Selected Repeats of Section 04B962**

<b>Visit</b>	<b>Repeat Numbers</b>					<b>Composite Correlation</b>
01	2	3	4	6	7	0.873
02	2	4	5	7	9	0.910
03	1	2	4	5	7	0.876
04	1	2	5	6	7	0.914
05	1	2	3	4	6	0.901
06	1	2	3	4	6	0.793
07	3	5	6	8	9	0.735
08	1	3	4	6	7	0.651

**Table 20. Selected Repeats of Section 04B964**

<b>Visit</b>	<b>Repeat Numbers</b>					<b>Composite Correlation</b>
01	1	2	4	5	6	0.914
02	2	5	7	8	9	0.934
03	1	2	5	6	7	0.878
04	1	2	4	5	6	0.888
05	1	2	5	6	7	0.883
06	2	3	6	7	9	0.937
07	1	5	7	8	9	0.833
08	1	2	4	6	9	0.728

The process for selecting five repeat measurements from a larger group is similar to the practice within LTPP except that it is based on composite agreement in profile rather than the overall index value. The correlation levels listed in Tables 13 through 20 provide an appraisal of the agreement between profile measurements for each visit of each section. When two profiles produce a correlation level above 0.82, their IRI values are expected to agree within 10 percent most (95 percent) of the time. Above this threshold, the agreement between profiles is usually acceptable for studying the influence of distresses on profile. When two profiles produce a correlation level above 0.92, they are expected to agree within 5 percent most of the time. Above this threshold, the agreement between profiles is good. Correlation above 0.92 often depends on consistent lateral tracking of the profiler and may be very difficult to achieve on highly distressed surfaces. The IRI values provided in this report will be the average of five observations, which will tighten the tolerance even further.

Overall, most of the groups of measurements in Tables 13 through 20 exhibited good or better correlation, and most exhibited acceptable correlation. Any group of repeat measurements that produced a composite correlation level below 0.82 was investigated using filtered plots; these results follow:

- Section 04B901, visit 07 and 08: Narrow downward spikes throughout the profiles significantly diminished the correlation.
- Section 04B902, visit 07: Narrow downward spikes throughout the left side profiles significantly diminished the correlation. These appeared in the same location in some, but rarely all, repeat measurements.
- Section 04B902, visit 08: Narrow downward spikes in isolated locations within the profiles significantly diminished the correlation.
- Section 04B903, visit 08: Narrow downward spikes in the left side profiles significantly diminished the correlation. These appeared in the same location in some, but rarely all, repeat measurements.

- Section 04B961, visit 08: Correlation was diminished by short-wavelength “noise” throughout the section on both the left and right side and several extraneous spikes in the left side profiles.
- Section 04B962, visits 06 through 08: Narrow downward spikes that rarely appeared in the same location in more than two repeat measurements significantly diminished the correlation.
- Section 04B964, visits 07 and 08: Correlation was diminished by short-wavelength “noise” throughout the section on both the left and right side.

## **SUMMARY ROUGHNESS VALUES**

Figures 17 through 24 show the left and right IRI values for each pavement section over its monitoring period. For most of the sections, this includes 14 summary IRI values: two per visit over seven visits. The figures show the IRI values versus time in years. In this case, “years” refers to the number of years between the measurement date and April 1, 1995. (All of the test sections were constructed in the second half of March 1995.) Fractions of a year are estimated to the nearest day.

To supplement the plots, the appendix to this report lists the IRI, Half-car Roughness Index (HRI), and Ride Number (RN) of each section for each visit. These roughness values are the average of the five repeat measurements selected in the data quality screening. These are not necessarily the same five repeat measurements selected for the LTPP database. The appendix also provides the standard deviation of IRI over the five repeat measurements to help identify erratic roughness values that result from transverse variations in profile caused by surface distresses.

Figures 17 through 24 provide a snapshot of the roughness history of each pavement section. The remainder of this chapter characterizes the profile content that made up the roughness and explains the profile features that contributed to roughness progression.

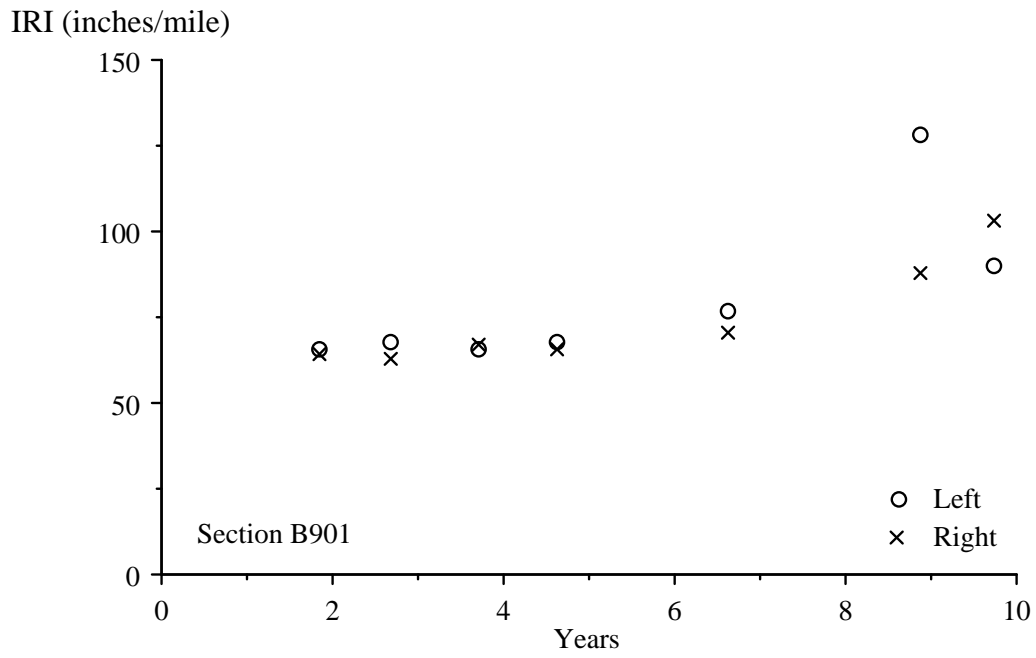


Figure 17. IRI Progression of Section 04B901

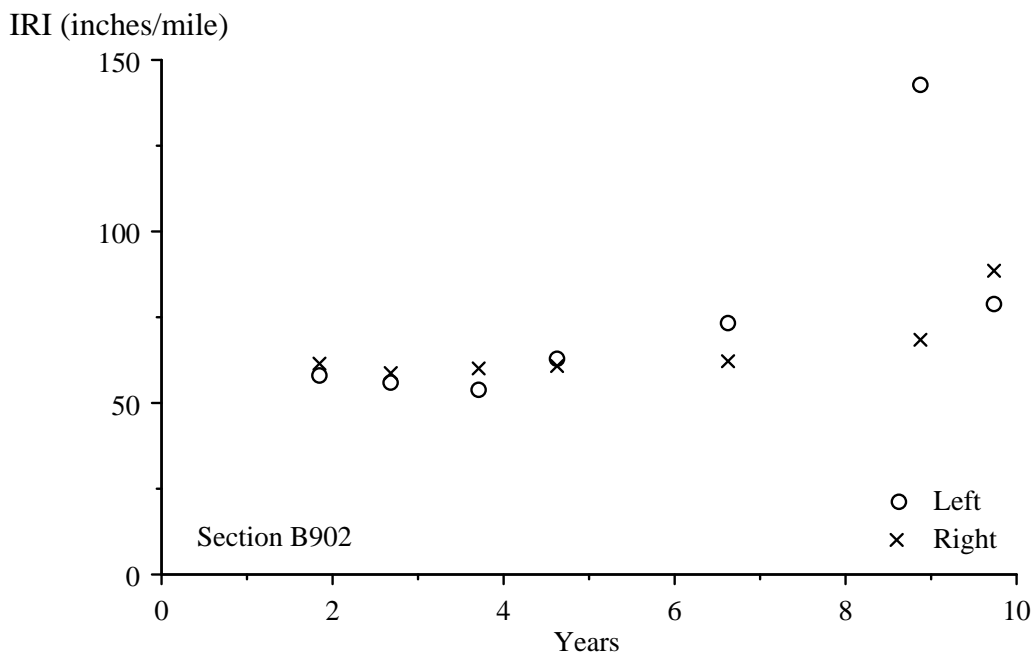


Figure 18. IRI Progression of Section 04B902

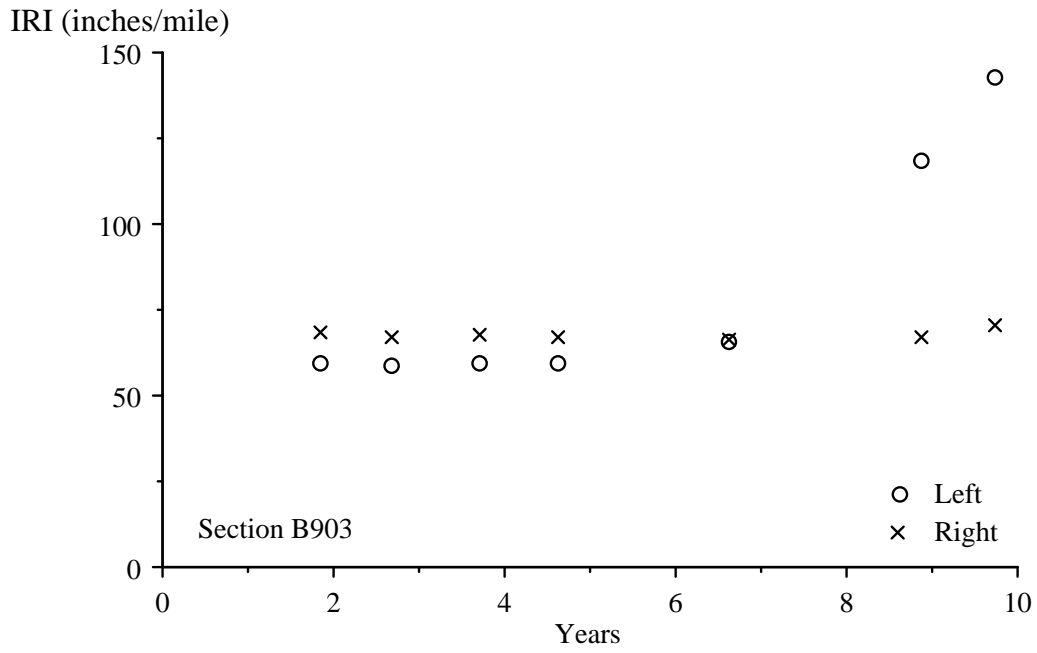


Figure 19. IRI Progression of Section 04B903

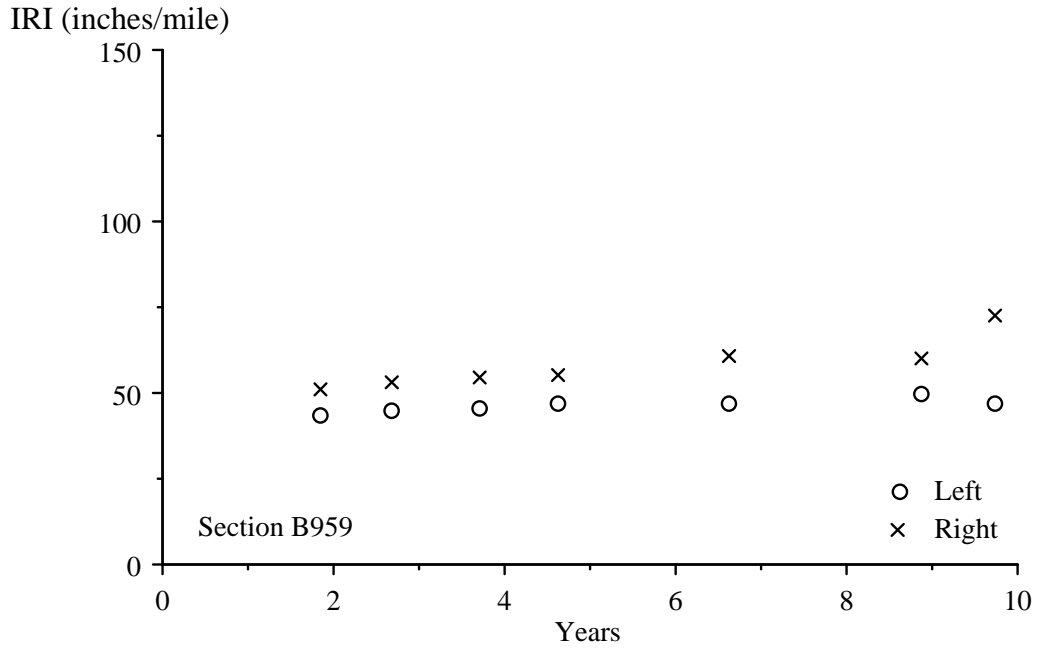
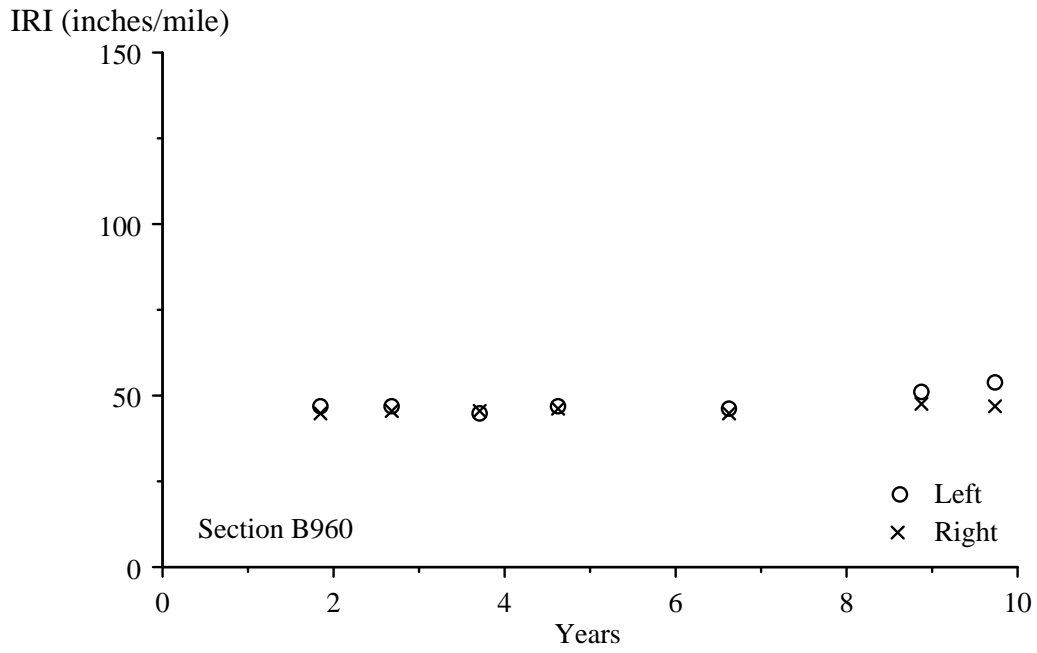
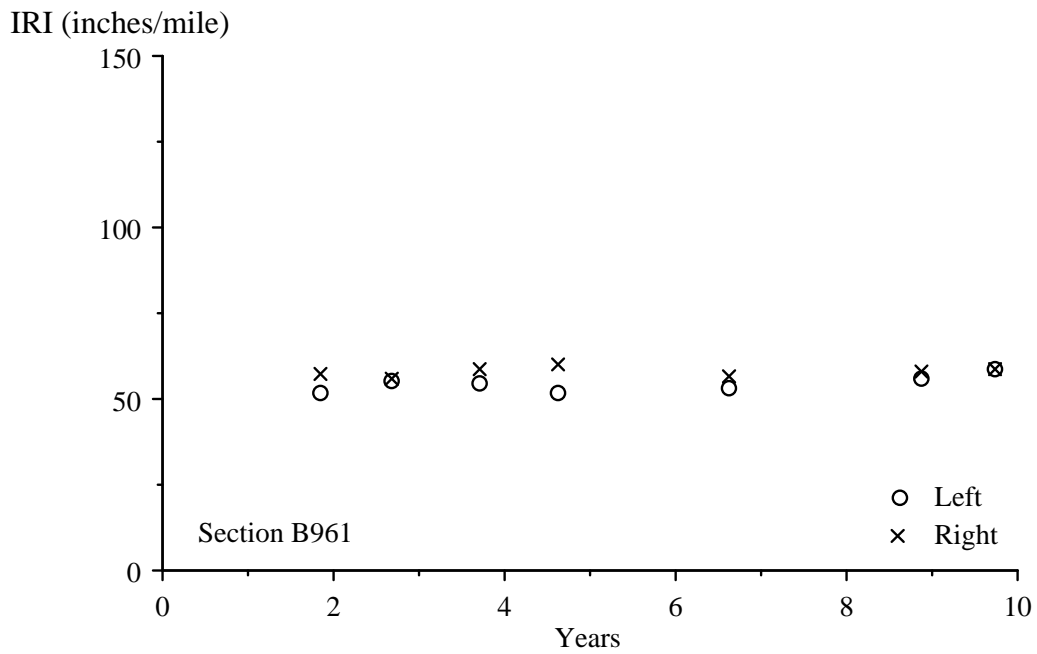


Figure 20. IRI Progression of Section 04B959



**Figure 21. IRI Progression of Section 04B960**



**Figure 22. IRI Progression of Section 04B961**

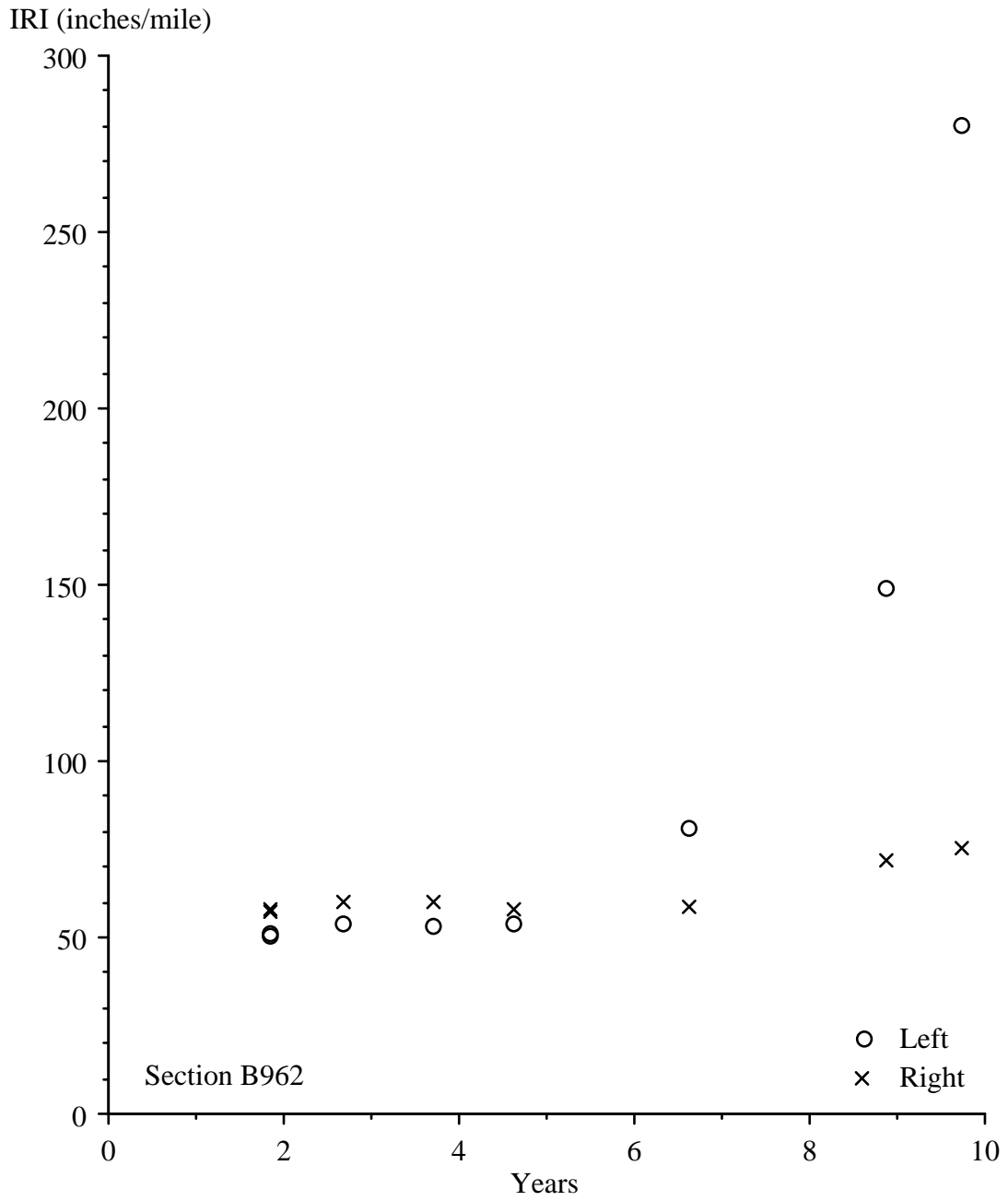
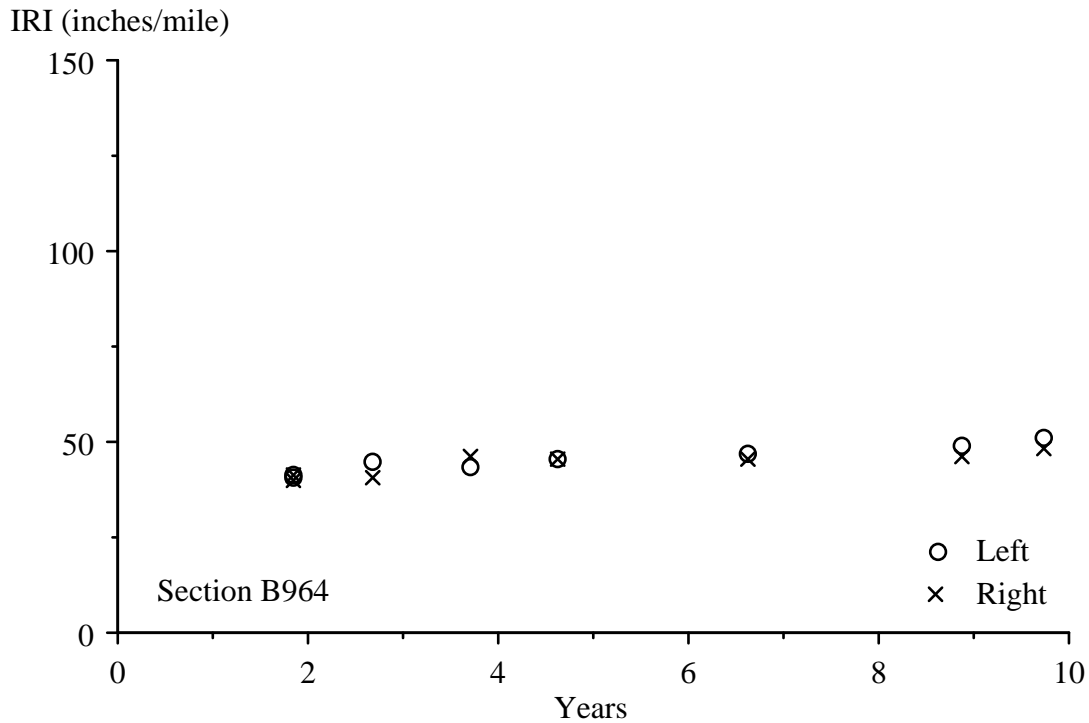


Figure 23. IRI Progression of Section 04B962



**Figure 24. IRI Progression of Section 04B964**

### PROFILE ANALYSIS TOOLS

Investigators used various analytical techniques to study the profile characteristics of each pavement section and their change with time. These tools help study roughness, roughness distribution, and roughness progression of each test section, including concentrated roughness that may be linked to pavement distress. The discussion of each analysis and plotting method is rather brief; Sayers and Karamihas (1996b) provide more details about these methods.

### Roughness Values

Investigators calculated left IRI, right IRI, Mean Roughness Index (MRI), HRI, and RN values. The appendix provides the average value of each index for each visit of each section. The discussion of roughness in this analysis emphasizes the left and right IRI. Nevertheless, comparing the progression of HRI and RN to the MRI provides additional information about the type of roughness that is changing. For example, a low HRI value relative to MRI indicates roughness that exists on only one side of the lane. Further, aggressive degradation of RN without a commensurate growth in MRI signifies that the developing roughness is biased toward short-wavelength content.

## Elevation Profile Plots

A simple way to learn about the type of roughness that exists within a profile is to view the trace. However, certain key details of the profile are often not as obvious in a raw profile trace as they may be after the profile is filtered. Three types of filtered plots were inspected for every visit of every section:

- Long wavelength: A profile smoothed with a base length of 25 ft and anti-smoothed with a base length of 125 ft.
- Medium wavelength: A profile smoothed with a base length of 5 ft and anti-smoothed with a base length of 25 ft.
- Short wavelength: A profile smoothed with a base length of 1 ft and anti-smoothed with a base length of 5 ft.

These filters were used to screen the profiles for changes with time and special features of interest. The terms “long,” “medium,” and “short” are relative, and in this case pertain to the relevant portions of the waveband that affects the IRI. The long-wavelength portion of the profile was typically very stable with time. However, the long-wavelength profile plots of every section changed somewhat between visit 06 and 07—not by a change in the surface characteristics of the section, but by a change in profiler make and the associated change in filtering practices.

The medium-wavelength plots provided a view of the features in a profile that were likely to have a strong effect on the IRI and may change with time. The short-wavelength elevation plots also typically progressed with time, but only affected the IRI through localized roughness or major changes in content with time. However, the short-wavelength elevation plots helped identify and track the progression of narrow dips and other short-duration features that may have been linked to distress.

In addition to filtered plots, every profile was viewed in its raw form. This helped reveal noteworthy features that did not necessarily affect the IRI, but helped establish a link between surface distress and profile properties. Two examples of this were narrow downward spikes in the profiles caused by cracking and deep, short-duration dips at potholes.

## Roughness Profile

A roughness profile provides a continuous report of road roughness using a given segment length (Sayers 1990). Instead of summarizing the roughness by providing the IRI for an entire pavement section, the roughness profile shows how IRI varies with distance along the section by using a sliding window to display the IRI of every possible segment of given base length along the pavement.

A roughness profile displays the spatial distribution of roughness within a pavement section. As such, it can be used to distinguish road sections with uniform roughness from sections with roughness levels

that change over their length. Further, the roughness profile can pinpoint locations with concentrated roughness and estimate the contribution of a given road disturbance to the overall IRI.

In this work, roughness profiles were generated and viewed using a base length of 25 ft, that is, every point in the plot shows the IRI of a 25-ft segment of road, starting 12.5 ft upstream and ending 12.5 ft downstream. Any location where a peak occurs in the roughness profile that is greater than or equal to 2.5 times the average IRI for the entire section is considered an area of localized roughness. All areas of localized roughness are discussed in the detailed observations by identifying them, listing their severity, and describing the underlying profile features that caused them.

### **Power Spectral Density Plots**

A power spectral density (PSD) plot of an elevation profile shows the distribution of its content within each waveband. An elevation profile PSD is displayed as mean square elevation versus wave number, which is the inverse of wavelength. PSD plots were calculated from the slope profile rather than the elevation profile, which aided in the interpretation of the plots because the content of a slope PSD typically covers fewer orders of magnitude than an elevation PSD.

A PSD plot is generated by performing a Fourier transform on a profile (or in this case, a slope profile). The PSD's value in each waveband is derived from the Fourier coefficients and represents the contribution to the overall mean square of the profile in that band.

The slope PSD plots provided a very useful breakdown of the content within a profile. In particular, the plots reveal (1) cases in which significant roughness is concentrated within a given waveband; (2) the type of content that dominates the profile (e.g., long, medium, or short wavelength); (3) the type of roughness that increases with time; and (4) the type of roughness that is stable with time.

For this project, the PSDs rarely provided much value beyond what was learned using filtered elevation plots and roughness profiles. However, any valuable observations that could be made from a PSD plot are discussed in the following section.

### **Distress Surveys**

Once the analysis and plotting were completed, all of the observations were compared to the manual distress surveys performed on each section. Manual distress survey results were available for each section on at least six dates over the monitoring history, starting in February 1995. These were performed using LTPP protocols by technicians certified to perform distress surveys. The surveys provided a means of relating profile features to known distresses.

### **DETAILED OBSERVATIONS**

This section reports key observations from the roughness index progression, filtered elevation profile plots, roughness profiles, PSD plots, and distress surveys. In many cases, similar behavior was noted for multiple sections. These observations are repeated under the heading of every section where

appropriate. However, changes in profile properties with time that were caused by changes in profiler make or model are summarized at the end of the report.

## **Section 04B901**

### *Roughness*

The IRI of the left side increased steadily from 66 to 90 inches/mi over the monitoring period, with the exception of a value of 128 inches/mi in visit 07. The IRI of the right side increased from 65 to 103 inches/mi over the monitoring period, but most of the increase occurred in the last two visits. The HRI was 11 percent to 14 percent below the MRI in visits 01 through 06, and was 19 percent to 21 percent below the MRI in visits 07 and 08.

### *Elevation Profile Plots*

The left side profiles were very consistent with each other over the first five visits. Visit 06 profiles were also consistent with previous visits in the medium- and long-wavelength range. However, the agreement in the short-wavelength range was not as good because of narrow downward spikes in some locations within the visit 06 profiles. By visit 07, a very high concentration of narrow downward spikes up to 0.5 inch deep appeared in the left side profiles over the entire length of the section. These sometimes appeared at the same location in more than one repeat measurement, but rarely appeared in all five. In visit 08, very few narrow downward spikes appeared in the profiles with the exception of a patch of spikes about 0.5 inch deep that occurred 5 to 10 ft and 37 to 39 ft from the start of the section.

The right side profiles were consistent with each other over the first six visits. (A minor exception was repeat 5 from visit 01, which was different from the others in the long-wavelength range.) Visit 07 profiles were very similar to those of previous visits except they included several narrow downward spikes that were rarely in the same location in more than one repeat measurement. The spikes appeared with the highest density in the last 140 ft of the section. Profiles from visit 08 included a much higher number of downward spikes over the entire section, and they were most prevalent in the first 100 ft of the section.

Two bumps stood out in the right side profiles from all seven visits. The first was about 115 ft from the start of the section and was 4 ft long and up to 0.15 inch high. The second was about 200 ft from the start of the section and was about 10 ft long and 0.2 inch high.

### *Roughness Profiles*

The left side roughness profiles were very consistent in visits 01 through 05. No localized roughness appeared in these visits, although the roughness was not particularly evenly distributed. The roughness was highest about 125 ft from the start of the section. This is near a series of four bumps up to 5 ft long and more than 0.1 inch high. The final bump in the series was about 131 ft from the start of the section. It was 5 ft long and over 0.2 inch high. By visit 08, the peak value of the roughness profiles in this location was 195 to 215 inches/mi.

In visits 06 and 07, the roughness profiles were not consistent with each other because of the hit-or-miss nature of the downward spikes within the elevation profiles.

The right side roughness profiles were fairly consistent with each other in visits 01 through 06. In visits 07 and 08, additional roughness appeared in every repeat measurement, but rarely in the same locations in any two repeats. Localized roughness appeared in all visits within the last 25 ft of the section. This area had peak roughness values of over 160 inches/mi in all visits. This roughness was caused by a series of disturbances about 5 ft long. (It is not clear if these are bumps or dips.) In visit 07 and one repeat measurement from visit 08, the peak roughness was much higher in this location because a narrow dip up to 1 inch deep appeared 480.5 ft from the start of the section in these profiles.

### *Distress Surveys*

WP cracking was first recorded in January 1999. This covered more than half of the left WP. By April 2002 cracking had covered all of the left WP, and longitudinal cracking covered about half of the right WP. In January 2005, areas of cracking covered both WPs over the entire length of the section. Transverse cracking was also recorded on both sides in multiple locations. (Ten feet of longitudinal distance without at least one transverse crack was rare.) Nothing in the distress surveys explain the localized roughness on the left side described above or the reduction in roughness on the left side between visits 07 and 08. The narrow dip 480.5 ft from the start of the section on the right side is in about the same location as a transverse crack recorded in April 2002 and January 2005.

## **Section 04B902**

### *Roughness*

The IRI of the left side did not follow a clear trend, but increased overall from 58 inches/mi in visit 01 to 79 inches/mi in visit 08. In visit 07, the left side IRI averaged 143 inches/mi, with a standard deviation of 28.1 inches/mi. These values were much higher than in any other visit. The IRI of the right side held steady between 59 and 63 inches/mi in visits 01 through 06, then increased to 89 inches/mi by visit 08. The HRI was 14 percent to 22 percent below the MRI.

### *Elevation Profile Plots*

The right side profiles were consistent in visits 01 through 06, and similar in visit 07. (A minor exception was repeat 5 from visit 01, which was different from the rest in the long-wavelength range.) A bump appears in the profiles of all visits from 195 to 203 ft that is about 0.2 inch high. The profiles from visit 08 include narrow downward spikes throughout the section. These often appear in only one repeat measurement in a given specific location, but some areas have a higher density of spikes than others.

The left side profiles were consistent in visits 01 through 05. (A minor exception was repeat 5 from visit 01, which was different from the rest in the long-wavelength range.) A patch of densely spaced narrow dips, up to 0.3 inch deep, appeared 120 to 145 ft from the start of the section in visit 05. Three new areas of densely spaced narrow dips appeared in the visit 06 profiles, from 215 to 235 ft, 305 to 330 ft, and 405 to 435 ft from the start of the section.

All visit 07 profiles included narrow downward spikes throughout the entire length of the section. These spikes were typically 0.4 inch or more deep and were poorly correlated among the five repeat measurements. Visit 07 profiles also included four bumps about a foot long: (1) about 120 ft from the start of the section, 0.5 inch high; (2) about 134 ft from the start of the section, 0.35 inch high; (3) about 304 ft from the start of the section, 0.2 inch high, detected in two repeats; and (4) about 307 ft from the start of the section, 0.3 inch high, detected in four repeats.

Visit 08 profiles included narrow dips in the same areas as visit 06 along with a few narrow downward spikes in other areas. None of the four bumps listed for visit 07 appeared in the visit 08 profiles. The patches of narrow dips in visit 08 were much more repeatable, isolated, and in some cases more severe than in previous visits.

### *Roughness Profiles*

An area of localized roughness appeared in the right side profiles about 197 ft from the start of the section in all visits. This was caused by the 8-ft-long bump described above. A peak also appeared in visits 01 through 07 of up to 140 inches/mi that is 120 ft from the start of the section. It was caused by a bump about 0.1 inch high from 113 to 117 ft from the start of the section. The right side roughness profiles from visit 08 were not very consistent because of the lack of repeatability in the appearance of the narrow downward spikes.

The roughness profiles from the left side included localized roughness in four of the five repeat measurements about 135 ft from the start of the section in visit 05. In visit 06, and particularly in repeat 6, the roughness profiles showed a significant increase over those of visit 05 in the areas where the narrow dips appeared. Visit 07 was much rougher than visit 06 in several areas, again because of the narrow dips. The roughness was highest in the first 150 ft of the section and in the last 100 ft (in repeat 7 only).

Visit 08 roughness profiles were much more repeatable on the left side than in visits 06 and 07. Areas of high roughness were centered about 125, 220, 315, and 420 ft from the start of the section.

### *Distress Surveys*

The patch of narrow dips in the left side profiles in visit 05 corresponds to an area of cracking recorded in the left WP in January 1999. This was the only cracking recorded in that survey. In April 2002, the distress survey recorded areas of cracking over most of the left WP and longitudinal cracking over much of the length of the section in the right WP.

Three of the four bumps listed for the left side profiles in visit 07 appear in locations where potholes were recorded in January 2005. The only pothole that was not in the vicinity of a corresponding bump was about 235 ft from the start of the section. In January 2005, potholes were detected in the left WP 121, 235, 305, 307, and 312 ft from the start of the section. These were locations where narrow dips were the most prevalent in visit 08 profiles, and all of these areas corresponded to peaks in the roughness profiles from visit 08.

## **Section 04B903**

### *Roughness*

The IRI of the left side increased from 59 to 66 inches/mi in visits 01 through 06, then increased to 143 inches/mi by visit 08. The IRI of the right side held steady between 67 and 71 inches/mi over the monitoring period. The HRI was 15 percent to 20 percent below the MRI.

### *Elevation Profile Plots*

In visit 06, narrow dips began to emerge in the left side profiles. They were up to 0.15 inch deep and appeared in the same location in more than one profile in some cases. Visit 07 profiles included more narrow dips on the left side. The dips were up to 0.5 inch deep, and the majority of them did not appear in the same location in multiple repeat measurements. Visit 08 included a much higher density of narrow dips. Many of the dips under 0.3 inch deep were not well repeated, but several deeper dips appeared at the same location in more than one repeat measurement.

Similar dips appeared in the right side profiles from visits 06 through 08, but not nearly as many, and they were much less severe.

A dip 1 ft long and at least 2.4 inches deep appeared in the left side profiles from visit 07 about 122 ft from the start of the section. A dip 1 ft long and 2 inches deep appeared in three of the five left side profiles from visit 08 about 333 ft from the start of the section.

### *Roughness Profiles*

The roughness was very uniform along the section on the left side in visits 03 and 04. In visit 06, the roughness was somewhat uniform along the section, but not very consistent among the repeat measurements. Severe localized roughness with a peak value of 540 inches/mi appeared in the location of the deep dip in visit 07. This feature alone added more than 25 inches/mi to the overall IRI of the left side. Severe localized roughness with a peak value of 630 to 695 inches/mi appeared about 333 ft from the start of the section in three of the five repeat measurements from visit 08. This accounted for about 30 inches/mi of additional roughness in those repeat measurements. It also explains the high (15.4 inches/mi) standard deviation among the left side IRI values.

No localized roughness was found in the right side profiles; they were very consistent with time in visits 01 through 07.

### *Distress Surveys*

No distress was recorded until April 2002 when longitudinal cracking and large areas of WP cracking were recorded. In January 2005, both WPs were covered with cracking over the entire length of the section. Nothing in the distress survey explains the deep dips in visits 07 and 08.

## **Section 04B959**

### *Roughness*

The IRI of the left side increased from 41 inches/mi in visit 01 to 47 inches/mi in visit 08 with a peak value of 50 inches/mi in visit 07. The IRI of the right side increased steadily from 51 to 73 inches/mi. The HRI was 13 percent to 16 percent below the MRI.

### *Elevation Profile Plots*

Profiles were very consistent over the monitoring period on the left side. The only feature that stood out was a dip at the start of the section 0.1-0.2 inch deep and about 10 ft long. The deepest part of the dip was only a few feet from the start of the section. Its shape was only fully developed in profiles that included lead-in, such as visits 07 and 08.

The right side profiles included narrow dips 188.5 ft from the start of the section in some of the repeat measurements from visits 04 and 05. But the profiles were fairly consistent in visits 01 through 07. In visit 08, several narrow dips up to 0.1 inch deep appeared, particularly in the first third of the section.

### *Roughness Profiles*

The roughness of the left side was uniform along the section with the exception of localized roughness at the very start of the section, which was caused by the long dip described above and roughness that appeared just ahead of the section start. The localized roughness only appeared in visits 07 and 08 because they included profiles upstream of the section start.

In the early visits, the roughness of the right side was uniform along the section. In later visits, and particularly in visit 08, most of the increase in roughness occurred in the first third of the section.

### *Distress Surveys*

Nothing in the distress surveys explains the narrow dip in visits 04 and 05. Very little distress was recorded before January 2005. By January 2005, significant cracking had appeared. Much of the cracking was found in the first third of the section along the right WP. This included transverse cracks and large areas of cracking within the WP. Narrow dips appeared in the visit 08 profiles in the position of most of the transverse cracks.

## **Section 04B960**

### *Roughness*

The IRI of the left side held steady between 45 and 47 inches/mi in visits 01 through 06, then increased to 54 inches/mi by visit 08. The IRI of the right side only ranged from 45 to 48 inches/mi. The HRI was 13 percent to 18 percent below the MRI.

### *Elevation Profile Plots*

The right side profiles were very consistent with time. Two small disturbances stood out in the medium-wavelength (and raw) profiles that were about 190 and 380 ft from the start of the section. The same features appeared on the left side, but they did not stand out among the roughness from the rest of the section. The left side profiles were very consistent with time in visits 01 through 06. In visit 07, a sunken area appeared 441 to 447 ft from the start of the section that included two dips within it, each at least 0.1 inch deep. In visit 08, this entire area was about 0.1 inch below the surrounding pavement, and it included three dips within it, each at least another 0.2 inch deep.

### *Roughness Profiles*

The right side roughness profiles were very consistent with time. In all visits, the roughness was about double the average near 190 and 380 ft from the start of the section. The left side roughness profiles were fairly consistent with time in visits 01 through 06. In visit 07, a peak of about 100 inches/mi appeared in the roughness profile about 445 to 450 ft from the start of the section. By visit 08, the same area showed peak roughness of up to 160 inches/mi. This localized roughness was caused by the sunken area with dips described above and was responsible for the majority of the increase in roughness of the entire section after visit 06.

### *Distress Surveys*

The distress surveys recorded very little distress before April 2002. Some transverse and longitudinal cracking was recorded in April 2002. This included longitudinal cracking from 435 to 450 ft from the start of the section on the left side of the lane and transverse cracking across the left WP about 443 and 447 ft from the start of the section. This corresponds to the sunken area and the dips within it described above. The distress survey from January 2005 observed cracking over the entire section in both WPs, but several transverse cracks in the area from 440 to 450 ft were also specifically recorded.

## **Section 04B961**

### *Roughness*

The IRI increased from 52 to 59 inches/mi on the left side, but the progression was not steady. The IRI only ranged from 56 to 60 inches/mi on the right side. The HRI was 10 percent to 12 percent below the MRI. This was the lowest difference observed for the SPS-9A project, and it is an unusually low difference for a full-depth asphalt pavement.

### *Elevation Profile Plots*

Profiles were very consistent over the monitoring period on both sides of the lane. They were unusually consistent with time in the short-wavelength range. Very few features stood out. One minor exception: a series of short (about 0.05 inch), narrow bumps 60 to 100 ft from the section start on both sides.

### *Roughness Profiles*

No localized roughness was detected on the left side, although the area from 60 to 100 ft from the start of the section was rougher than the rest. On the right side, a peak value of up to 140 inches/mi appeared about 95 ft from the start of the section. This localized roughness was caused by the bumps described above.

### *Distress Surveys*

Nothing in the distress surveys directly explains the series of narrow bumps observed in the profiles. Very little distress was observed before the final survey in January 2005. That survey recorded a significant amount of raveling, particularly on the left side of the lane.

## **Section 04B962**

### *Roughness*

The IRI of the left side held steady between 51 and 54 inches/mi in visits 01 through 05, then increased rapidly to 281 inches/mi in visit 08. The IRI of the right side held steady between 58 and 61 inches/mi in visits 01 through 06, then increased to 76 inches/mi by visit 08. The HRI was 13 percent to 17 percent below the MRI.

### *Elevation Profile Plots*

Profiles from the left side were consistent over visits 01 through 05, and profiles from the right side were very consistent over visits 01 through 06. Those profiles included areas with small bumps 2 to 5 ft long from 180 to 210 ft and 360 to 420 ft from the start of the section on both sides.

The right side profiles included several narrow downward spikes throughout the section in visits 07 and 08. Heavy concentrations of these spikes appeared 162 to 172 ft, 230 to 245 ft, 295 to 305 ft, 355 to 365 ft, and 475 ft from the start of the section. (These account for the additional roughness compared to visits 01 through 06.)

In visit 06, the left side profiles included narrow downward spikes in the ranges from 60 to 80 ft, 150 to 180 ft and 410 to 440 ft from the start of the section. The dips often appeared in the same location in more than one repeat measurement, but rarely in all five. The deepest, and most well repeated, dip was less than 1 ft long, up to 1.4 inch deep, and appeared 430 ft from the start of the section.

In visit 07, the left side profiles included narrow downward spikes up to 1 inch deep over the entire section. They usually appeared in the same location in more than one repeat measurement, but not in all repeats. The highest concentration of downward spikes appeared between 360 and 450 ft from the start of the section. In one repeat measurement, a dip 0.5 ft long and 0.8 inch deep appeared 170 ft from the start of the section. In two other repeat measurements, a dip appeared 80 ft from the start of the section that was 0.5 ft long and at least 0.7 inch deep.

The visit 07 profiles from the left side also included five longer disturbances that were detected in all five repeat measurements: (1) a 2 ft long, 0.5 inch deep dip centered 418 ft from the start of the section; (2) a 4 ft long, 0.5 inch deep dip centered 431 ft from the start of the section; (3) a 1.5 ft long, 0.4 inch high bump 471 ft from the start of the section; (4) a 2 ft long, 0.4 inch high bump 484 ft from the start of the section; and (5) a 1.5 ft long, up to 0.3 inch high bump 492 ft from the start of the section. All of these features appeared among a high concentration of narrow downward spikes.

The visit 08 profiles from the left side included many areas with a high concentration of narrow downward spikes up to 2.5 inches deep, but the spikes rarely appeared in more than the same location in more than two repeat measurements. The highest concentration of spikes appeared in repeats 4 and 7. The profiles also included some bumps up to 2 ft long and 0.5 inch high in the last 40 ft of the section and a 4 ft long, 0.5 inch deep dip in the last 5 ft of the section.

### *Roughness Profiles*

Roughness profiles for the right side were very consistent in visits 01 through 06. Although no localized roughness appeared in these profiles, the distribution of roughness along the section was not very uniform. The growth in roughness after visit 06 took place over the entire length of the section.

No localized roughness was detected on the left side in visits 01 through 06, although the areas with small bumps described above were rougher than the surrounding pavement.

In visits 06 and 07, localized roughness (or at least increased roughness) in the left side profiles appeared about 80 ft from the start of the section in one repeat measurement per visit and about 175 ft from the start of the section in one or two repeat measurements per visit. These are locations where deep, narrow dips were found in some, but not all, repeat measurements. Localized roughness also appeared in visit 06 about 430 ft from the start of the section and in the last 20 ft of the section. Both of these areas appeared as severe localized roughness in visit 07, with peak values of up to 550 inches/mi in the roughness profiles.

In visit 08, the left side profiles were very rough over much of the section. (The exception was the area from 230 to 350 ft from the start of the section.) The most severe localized roughness appeared (1) at the very end of the section; (2) in one repeat measurement about 20 ft from the start of the section; and (3) in all but one repeat measurement about 80 ft from the start of the section.

### *Distress Surveys*

The distress survey of January 1999 showed five areas of longitudinal cracking or WP cracking. Many of these areas correspond to the locations where narrow downward spikes appeared in the left side profiles from visit 06. In visits 07 and 08, cracking covered the entire left WP (and most of the right WP). This probably explains the downward spikes that appeared throughout the profiles and the hit-or-miss nature of their distribution.

The distress survey in April 2002 recorded potholes about 427 ft and 434 ft from the start of the section. The distress survey in January 2005 recorded a large number of potholes and patches in the left WP over

the last 100 ft of the section. Their locations corresponded to the locations of longer bumps and dips in the visit 07 and 08 profiles.

The deep narrow dip in the left side profiles from visits 06 through 08 did not correspond to anything in the distress surveys beyond the WP cracking found over the entire section.

#### **Section 04B964**

##### *Roughness*

The IRI increased fairly steadily from 41 to 52 inches/mi on the left side and from 42 to 49 inches/mi on the right side. The HRI was 11 percent below the MRI in visit 01. The gap between HRI and MRI grew steadily to 17 percent by visit 08.

##### *Elevation Profile Plots*

The profiles changed very little over the monitoring period with the exception of three rough features.

- After visit 02, a dip appeared about 136 ft from the start of the section on the left side. It was about 1 ft long and grew in depth from 0.15 inch to 0.4 inch over visits 03 through 08. However, the dip was not present in every repeat measurement.
- A dip up to 0.15 inch deep appeared 155 ft from the start of the section's left side in all visits.
- Starting in visit 04, a narrow dip appeared in the right side profiles about 160 ft from the start of the section. The dip rarely appeared in all five repeat measurements within a visit and ranged in depth up to 0.25 inch.

##### *Roughness Profiles*

Together, the first two dips described above caused an area of localized roughness that grew in severity to a peak value of 130 inches/mi by visit 08. The increased roughness at this area contributed significantly to the growth in roughness with time on the left side between visits 01 and 07.

In the most extreme case (visit 04, repeat 01), the third dip described above caused a peak value in the roughness profile of 106 inches/mi on the right side. Other than the influence of the dip 160 ft from the start of the section, roughness was very evenly distributed along the section on the right side.

##### *PSD Plots*

Although the content was biased toward long wavelengths, some content was isolated around wavelengths of about 15 to 16 ft on the left side.

## *Distress Surveys*

Nothing in the distress surveys directly explains the three narrow dips described above. Very little distress was observed before April 2002. In April 2002 and January 2005, the distress surveys recorded raveling along the entire section in both WPs.

### **SUMMARY**

This section summarizes important observations from each pavement section within the SPS-9A project limits. Some observations within this report were common to more than one pavement section, as described below. This section of the report, in conjunction with the roughness progression plots (Figures 17 through 24), provides the essential information about each pavement section.

Profiles from Sections 04B901, 04B902, 04B903, and 04B962 included narrow downward spikes dispersed throughout their length. The spikes usually appeared in only one or two repeat measurements at each location. These were caused by cracking, which covered both WPs of Sections 04B901, 04B902, 04B903, and 04B962 in the later visits. The spikes typically first appeared in profile measurements from November 2001 (visit 06), but were much more prevalent in February and December 2004 (visits 07 and 08). The spikes were usually more severe and numerous in the left side profiles. In Sections 04B901 and 04B902, the spikes were most severe in the left side profiles from visit 07. Although it is not clear why fewer spikes were detected in visit 08 on those two sections, it may be a consequence of a subtle difference in profiler positioning. The spikes account for most of the increase in the IRI values, particularly on the left side, in Sections 04B901, 04B902, 04B903, and 04B962 after November 2001.

Sections 04B902 and 04B962 included several potholes in the left WP that were observed in the distress survey from January 2005. The profiles in the location of these potholes were rarely consistent among the five repeat measurements from the last two profiling visits. In Section 04B902, the narrow downward spikes found throughout the profiles were somewhat more likely to appear near the potholes than in other locations, but no direct relationship was observed. Bumps appeared near two of the potholes in two of the five repeat profile measurements in February 2004. This may have been caused by narrow patching that was only covered by the lateral placement of the profiler in two of the passes, but no patching was noted. In Section 04B962, two of the seven potholes caused dips about 0.5 ft long and up to 1 inch deep in the last profiling visit that were fairly well repeated.

The final distress survey (January 2005) for Sections 04B901, 04B902, 04B903, 04B960, 04B962, and 04B964 all showed areas of cracking that cover both WPs over the entire section length. In these instances, fatigue cracking is so prevalent that it is difficult to match individual cracks to roughness within the measured profile. However, in a few cases, features in the profiles that affected the roughness were found that correspond directly to the location of transverse cracks noted in the distress survey. Several narrow dips appeared in Section 04B959 in the final profiling visit that corresponded to the locations of transverse cracks noted in January 2005. In Section 04B901, a narrow dip appeared in the right side profiles about 480 ft from the start of the section in the last two profiling visits. This is a location where transverse cracking was noted in April 2002. An area of localized roughness about 10 ft long appeared in the last two visits of Section 04B960 that included multiple transverse cracks.

## **Profiler Model**

The change in profiler in late 2002 affected the long-wavelength content of the profiles on every test section because the newer profiler used a high-pass filter that eliminated a little more of the profile content than the previous device. The change in high-pass filtering methods had no probable effect on the measurement of localized roughness or the study of narrow bumps and dips caused by distresses.

Another minor device effect within the profiles was peaks in the PSD plots with no pavement-related explanation. In visits 01 through 06 (measured by the K.J. Law Engineers T-6600 profiler), all profiles from the left and right side included a peak in their spectral content at a wavelength somewhere between 0.35 and 0.52 ft and another at a wavelength of double the first.

## **Individual Test Sections**

The summaries below provide the most important observations made about each test section. To help provide context for these summary statements, Figure 25 shows the range of left and right IRI for each section. Note that the highest IRI value for some of the sections did not occur in the final visit. (See the appendix or Figures 17 through 24.)

### *Section 04B901*

Although this section started out moderately smooth, with an MRI value of 65 inches/mi, roughness grew significantly to a final MRI value of 97 inches/mi. While the roughness of the right side grew steadily, the roughness of the left side reached a peak IRI value of 128 inches/mi in February 2004 and then reduced to a final value of 90 inches/mi. In the last three profiling visits, the profiles included narrow downward spikes that often did not appear in the same location in more than one repeat measurement. The highest concentration of dips appeared in the left side profiles in February 2004, which accounts for much of the additional roughness over the previous and subsequent visits. Localized roughness appeared in the right side profiles over the last 25 ft of the section because of 5-ft-long bumps and dips. In 2004, the profiles in this area also often included a 1-inch deep narrow dip at a transverse crack 480.5 ft from the start of the section.

### *Section 04B902*

The section was somewhat smooth until 2004. Starting with the profile measurement of November 2001, the profiles included an increasing number of narrow dips, particularly on the left side, that often did not appear in the same location in more than one repeat measurement. These dips were most severe in the left side profiles from February 2004, which had an average roughness value of 143 inches/mi, but were not at all consistent with each other. Although the spikes were less severe in November 2004, the profiles included patches of narrow dips in three areas where potholes were recorded in the distress surveys.

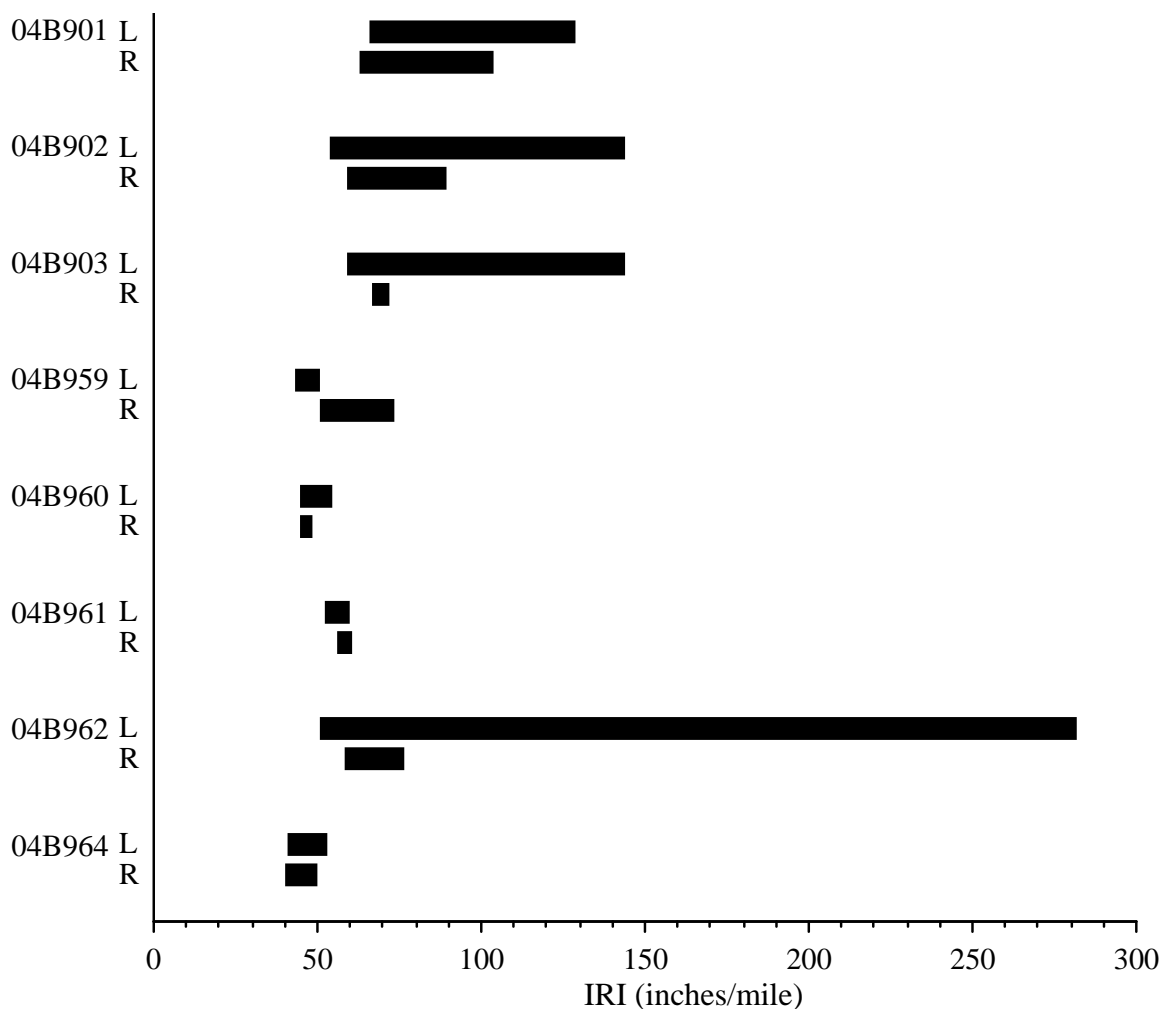


**Figure 25. Summary of IRI Ranges**

*Section 04B903*

The right side of this section remained somewhat smooth throughout the monitoring history, but the left side IRI more than doubled between visits 06 and 08. Starting in visit 06, the profiles included an increasing number of narrow dips, particularly on the left side, that often did not appear in the same location in more than one repeat measurement. In visit 07, a deep (2.4-inch) narrow dip appeared 122 ft from the start of the section on the left side. A deep (2-inch) narrow dip appeared 333 ft from the start of the section in three of the five repeat measurements from visit 08 on the left side. Both dips caused severe localized roughness. Roughness at the dip in visit 08 accounted for the high (15.4 inches/mi) standard deviation in the left side IRI from visit 08.

#### *Section 04B959*

This section remained smooth throughout the monitoring period, although the MRI progressed by 13 inches/mi. An area of localized roughness appeared on the left side at the start of the section because of a long dip and some rough features just ahead of the section start. The roughness of the right side was uniform along the section, until the roughness progressed significantly in the first third of the section because of the influence of cracking.

#### *Section 04B960*

The MRI increased from 46 to 51 inches/mi over the monitoring period. An area of localized roughness appeared on the left side about 445 ft from the start of the section by the end of the monitoring period. A sunken area of pavement, including three narrow dips about 0.2 inch deep at transverse cracks, caused the roughness. This area accounts for most of the roughness progression of the entire section.

#### *Section 04B961*

The MRI ranged from 55 to 59 inches/mi over the entire monitoring period. An area of increased roughness appeared on the right side of the lane 60 to 100 ft from the start of the section because of a series of short, narrow bumps in the profiles. The bumps appeared on the left side of the lane also, but they did not increase the roughness as much there. The bumps were very consistently measured over the monitoring period.

#### *Section 04B962*

This section remained smooth until 2004, when the final MRI value was 178 inches/mi, more than three times the initial value of 55 inches/mi. The sharp increase in roughness occurred primarily within the left side profiles. By the final visit, the left side profiles were strongly affected by roughness at potholes and patching, and included a high concentration of deep, narrow downward spikes caused by cracking in the WP. Most of the potholes and patches appeared in the last 100 ft of the section.

#### *Section 04B964*

The MRI increased from 41 to 50 inches/mi over the monitoring period. The majority of the roughness progression on this section was caused by three narrow dips that grew in severity with time: (1) 136 ft from the start of the section on the left side, (2) 155 ft from the start of the section on the left side, and (3) 160 ft from the start of the section on the right side.



## CHAPTER 5. CONCLUSIONS AND RECOMMENDATIONS

ADOT initiated the SPS-9A project to study the relative performance of the Superpave binders compared to the commonly used agency binders, which will provide a foundation for future design decisions. Surface distress, deflection, and profile data were used as the basis for performance evaluation and were analyzed as part of the study.

The SPS-9A project offers a unique opportunity to directly compare performance of various asphalt binders while reducing the confounding effect of other variables such as traffic-loading, climate, and subgrade conditions. However, findings drawn from this evaluation must be considered carefully. The experiment design did not offer replicate treatments to verify findings. Conclusions drawn from this comparison are based on one set of in situ conditions; observations from other climate or loading scenarios may differ from those noted within this report. Therefore, findings reported may be unique to the conditions and construction of this site.

Despite these issues, the data captured at the project provides valuable insight into pavement performance, design, management, and construction. Following is a summary of lessons learned from the performance data collected at the SPS-9A site:

- Roughness and roughness progression alone cannot be used to represent the health of a test section. Several test sections did not exhibit changes in roughness in proportion to the amount of fatigue cracking, and sections that had clearly reached the end of their service lives did not necessarily have roughness values that would trigger a rehabilitation event.
- Most every section except Section 04B959 (SMA polymer with ACFC) and Section 04B961 (SMA polymer with cellulose) showed significant growth in fatigue and longitudinal cracking 10 years after construction.
- Where fatigue cracking was very prevalent, it was difficult to match individual cracks to roughness within the measured profile. However, in a few cases, features in the profiles that affected the roughness corresponded directly to the location of transverse cracks noted in the distress survey.
- Construction quality can play a major role in performance. The construction observations documented in the LTPP construction report were limited to Superpave sections (Sections 04B902 and 04B903) and the agency standard mix section (Section 04B901). However, it showed that all three sections were free of any construction issues.
- Half of the sections (04B901, 04B959, 04B960, 041007/04B962) had reasonable patterns of environmental distress growth with a clear increase in magnitude approximately 10 years after construction. Section 04B964 had little environmental distress growth for seven years and then rapidly increased after 10 years.

- With no replicate sections, researchers had limited ability to assess potential variability independent of actual performance.
- For the SP-1 mix designs (Sections 04B902 and 04B903), the PG 70-10 binder (Section 04B903) performed significantly better, both structurally and environmentally, than the PG 76-10 binder (Section 04B902). It also performed significantly better than the standard agency mix at resisting environmental deterioration.
- All sections performed well with regard to rut resistance. Rutting would not have triggered a rehabilitation event for any section.
- SMA with cellulose fibers was, by far, the best pavement mix at resisting both structural and environmental deterioration. From a roughness perspective, the SMA and ARAC sections outperformed the Superpave mixes.

Based on these findings, the research team recommends the following:

- Most of the pavement test sections appeared to have experienced top-down cracking; however, this could not be confirmed. It is recommended that forensic analysis be performed at other locations throughout Arizona to learn about the factors contributing to top-down cracking.
- If the SMA with cellulose is sufficiently cost-effective, ADOT should consider expanding its use in overlay applications.

## REFERENCES

- American Association of State Highway and Transportation Officials (AASHTO). 1993. *AASHTO Guide for Design of Pavement Structures*. Washington, D.C.: American Association of State Highway and Transportation Officials.
- Evans, L. D. and A. Eltahan. 2000. *LTPP Profile Variability*. Publication FHWA-RD-00-113. McLean, VA: Federal Highway Administration: 178.
- Federal Highway Administration (FHWA). 1998. "Arizona SPS-9, I-10 Westbound Milepost 112-123, Construction Report on Site 04B900, Arizona Department of Transportation, Final."
- Huang, Y. H. 1993. *Pavement Analysis and Design*. Englewood Cliffs, NJ: Prentice-Hall.
- Karamihas, S. M. 2004. "Development of Cross Correlation for Objective Comparison of Profiles." *International Journal of Vehicle Design* 36(2/3): 173–193.
- Karamihas, S. M., T. D. Gillespie, and S. M. Riley. 1995. "Axle Tramp Contribution to the Dynamic Wheel Loads of a Heavy Truck." *Proceedings of the 4th International Symposium on Heavy Vehicle Weights and Dimensions*, Ann Arbor, MI. C. B. Winkler (ed.): 425–434.
- Kim, Y. Richard, B. Underwood, M. Sakhaei Far, N. Jackson, and J. Puccinelli. 2011. *LTPP Computed Parameter: Dynamic Modulus*. Publication FHWA-HRT-10-035. Washington, D.C.: Federal Highway Administration.
- Mahoney, J. 1995. *WSDOT Pavement Guide, Volume 2: Pavement Notes*. Olympia: Washington State Department of Transportation.
- Miller, J. S. and W. Y. Bellinger. 2003. *Distress Identification Manual for the Long-Term Pavement Performance Program*. Revised fourth edition. Publication FHWA-RD-03-031. Washington, D.C.: Federal Highway Administration.
- Rada, G. R., C. L. Wu, R. K. Bhandari, A.R. Shekharan, G. E. Elkins, and J. S. Miller. 1999. *Study of LTPP Distress Data Variability, Volume I*. Publication FHWA-RD-99-074. Washington, D.C.: Federal Highway Administration.
- Sayers, M. W. 1989. "Two Quarter-Car Models for Defining Road Roughness: IRI and HRI." *Transportation Research Record: Journal of the Transportation Research Board* 1215: 165–172.
- Sayers, M. W. 1990. "Profiles of Roughness." *Transportation Research Record: Journal of the Transportation Research Board* 1260: 106–111.
- Sayers, M. W. and S. M. Karamihas. 1996a. "Estimation of Rideability by Analyzing Longitudinal Road Profile." *Transportation Research Record: Journal of the Transportation Research Board* 1536: 110–116.

Sayers, M. W. and S. M. Karamihas. 1996b. *Interpretation of Road Roughness Profile Data*. Publication FHWA-RD-96-101 (Washington, D.C.: Federal Highway Administration): 177.

Simpson, A. L. 2001. *Characterization of Transverse Profiles*. Publication FHWA-RD-01-024. Washington, D.C.: Federal Highway Administration.

## APPENDIX: ROUGHNESS VALUES

This appendix lists the left International Roughness Index (IRI), right IRI, mean roughness index (MRI), Half-car Roughness Index (HRI), and Ride Number (RN) values for each visit of each section. The roughness values are the average for five repeat runs. The five runs were selected from a group of as many as nine by automated comparison of profiles, as described in the report. Values of standard deviation are also provided for left and right IRI to reveal cases of high variability among the five measurements. However, the screening procedure used to select five repeats usually helped reduce the level of scatter.

The discussion of roughness in the report emphasizes the left and right IRI. Nevertheless, the other indexes do provide useful additional information. MRI is simply the average of the left and right IRI value. HRI is calculated by converting the IRI filter into a half-car model (Sayers 1989) by collapsing the left and right profile into a single profile in which each point is the average of the corresponding left and right elevation. The IRI filter is then applied to the resulting signal. The HRI is very similar to the IRI except that side-to-side deviations in profile are eliminated. The result is that the HRI value for a pair of profiles will always be lower than the corresponding MRI value. Comparing the HRI and MRI value provides a crude indication of the significance of roll (i.e., side-by-side variation in profile) to the overall roughness. When HRI is low compared to MRI, roll is significant. This is common among asphalt pavements (Karamihas et al. 1995). Certain types of pavement distress, such as longitudinal cracking, may also cause significant differences between HRI and MRI.

Figure 26 compares the HRI to MRI for all of the profile measurements that are covered in this appendix (290 pairs of roughness values). The figure shows a best fit line with a zero intercept and a line of equality. The slope of the line is 0.845, which is typical for asphalt pavement.

RN has shown a closer relationship to road user opinion than the other indexes (Sayers and Karamihas 1996a). As such, it may help distinguish the segments from each other by ride quality. Further, the effect on RN may help quantify the impact of that distress on ride when a particular type of distress dominates the roughness of a section. In particular, a very low RN value coupled with moderate IRI values indicates a high level of short wavelength roughness and potential sensitivity to narrow dips and measurement errors caused by coarse surface texture.

Table 21 provides the roughness values. The table also lists the date of each measurement and the time in years since the site was opened to traffic. Negative values indicate measurements that were made before rehabilitation.

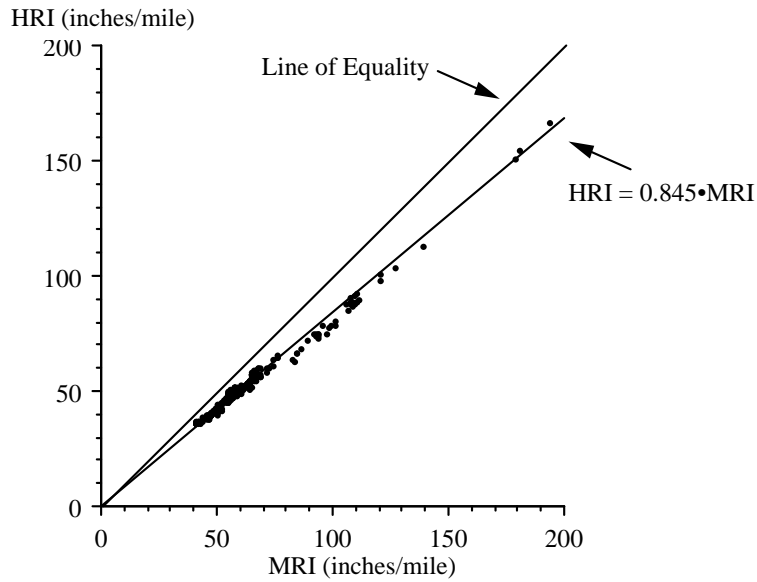


Figure 26. Comparison of HRI to MRI

Table 21. Roughness Values

Section	Date	Years	Left IRI (inch/mi)		Right IRI (inch/mi)		MRI (inch/mi)	HRI (inch/mi)	RN
			Ave	St Dev	Ave	St Dev			
04B901	29-Jan-97	1.84	66	1.0	65	1.2	65	58	3.79
04B901	5-Dec-97	2.68	68	1.5	63	1.5	65	57	3.67
04B901	7-Dec-98	3.69	66	1.1	68	1.2	67	59	3.68
04B901	10-Nov-99	4.61	68	1.0	66	1.9	67	58	3.72
04B901	12-Nov-01	6.62	77	2.1	70	2.1	74	63	3.51
04B901	9-Feb-04	8.86	128	4.9	88	4.2	108	88	2.41
04B901	17-Dec-04	9.71	90	4.2	103	4.1	97	77	2.82
04B902	29-Jan-97	1.84	58	1.3	61	1.4	60	50	3.87
04B902	5-Dec-97	2.68	56	1.6	59	1.1	58	49	3.82
04B902	7-Dec-98	3.69	54	0.8	61	0.5	58	49	3.82
04B902	10-Nov-99	4.61	63	3.1	61	0.7	62	53	3.68
04B902	12-Nov-01	6.62	73	10.3	63	0.6	68	57	3.46
04B902	9-Feb-04	8.86	143	28.1	69	2.9	106	86	2.56
04B902	17-Dec-04	9.71	79	2.3	89	0.6	84	66	2.94
04B903	29-Jan-97	1.84	59	0.6	69	1.1	64	54	3.77
04B903	5-Dec-97	2.68	59	1.8	67	0.5	63	53	3.71
04B903	7-Dec-98	3.69	60	0.5	68	1.0	64	54	3.73
04B903	10-Nov-99	4.61	60	0.9	68	1.0	64	53	3.80
04B903	12-Nov-01	6.62	66	3.2	67	1.3	66	54	3.69
04B903	9-Feb-04	8.86	119	1.8	68	1.9	93	75	2.37
04B903	17-Dec-04	9.71	143	15.4	71	2.9	107	87	2.42

**Table 21. Roughness Values (Continued)**

Section	Date	Years	Left IRI (inch/mi)		Right IRI (inch/mi)		MRI (inch/mi)	HRI (inch/mi)	RN
			Ave	St Dev	Ave	St Dev			
04B959	29-Jan-97	1.84	43	0.6	51	0.7	47	41	4.22
04B959	5-Dec-97	2.68	45	0.6	53	0.7	49	43	4.08
04B959	7-Dec-98	3.69	46	0.5	55	0.8	50	44	4.09
04B959	10-Nov-99	4.61	47	0.5	55	1.1	51	44	4.13
04B959	12-Nov-01	6.62	47	0.6	61	1.1	54	46	4.10
04B959	9-Feb-04	8.86	50	0.9	60	1.4	55	46	3.95
04B959	17-Dec-04	9.71	47	1.1	73	4.2	60	51	3.81
04B960	29-Jan-97	1.84	47	1.1	45	0.9	46	39	4.07
04B960	5-Dec-97	2.68	47	0.6	46	0.7	46	39	3.95
04B960	7-Dec-98	3.69	45	1.0	46	0.8	46	39	3.99
04B960	10-Nov-99	4.61	47	0.7	46	0.6	47	40	4.05
04B960	12-Nov-01	6.62	46	0.6	45	0.4	46	40	4.06
04B960	9-Feb-04	8.86	52	0.7	48	0.7	50	41	3.75
04B960	17-Dec-04	9.71	54	1.3	47	1.1	51	42	3.66
04B961	29-Jan-97	1.84	52	0.3	58	0.6	55	49	4.00
04B961	5-Dec-97	2.68	56	0.8	56	0.6	56	50	3.86
04B961	7-Dec-98	3.69	55	1.5	59	1.7	57	51	3.88
04B961	10-Nov-99	4.61	52	1.0	60	0.9	56	50	3.99
04B961	12-Nov-01	6.62	54	1.1	57	0.4	55	50	3.97
04B961	9-Feb-04	8.86	56	1.1	58	0.4	57	51	3.82
04B961	17-Dec-04	9.71	59	2.8	59	1.3	59	52	3.77
04B962	29-Jan-97	1.83	52	1.9	59	2.0	55	48	3.84
04B962	2-Feb-97	1.84	51	1.0	58	0.7	54	47	3.86
04B962	5-Dec-97	2.68	54	2.0	60	0.9	57	50	3.71
04B962	7-Dec-98	3.69	53	1.4	61	1.6	57	49	3.73
04B962	10-Nov-99	4.61	54	1.7	58	0.9	56	49	3.79
04B962	12-Nov-01	6.62	81	5.5	59	1.1	70	58	3.06
04B962	9-Feb-04	8.86	149	12.3	72	1.8	111	92	2.26
04B962	17-Dec-04	9.71	281	49.8	76	3.0	178	152	1.77
04B964	29-Jan-97	1.83	41	0.3	42	0.9	41	37	4.24
04B964	2-Feb-97	1.84	41	0.8	40	0.5	41	36	4.23
04B964	5-Dec-97	2.68	45	1.2	41	0.5	43	37	4.02
04B964	7-Dec-98	3.69	44	0.4	47	1.5	45	38	4.03
04B964	10-Nov-99	4.61	46	0.8	46	1.4	46	39	4.02
04B964	12-Nov-01	6.62	47	0.8	46	0.6	47	40	4.01
04B964	9-Feb-04	8.86	49	1.4	47	1.1	48	41	3.79
04B964	17-Dec-04	9.71	52	1.8	49	2.4	50	41	3.76





